DEFENCE S&T TECHNICAL BULLETIN

BULETIN TEKNIKAL S&T PERTAHANAN

VOL. / JIL. 1 | NO. / BIL. 1 | YEAR / TAHUN 2008 | ISSN 1985-6571

CONTENTS

STRIDE

SCIENCE & TECHNOLOGY RESEARCH INSTITUTE FOR DEFENCE
INSTITUT PENYELIDIKAN SAINS & TEKNOLOGI PERTAHANAN

ISSN 1985-6571

AIMS AND SCOPE

The Technical Defence S&T Bulletin (*Buletin Teknikal S&T Pertahanan*) is the official techinal bulletin of the Science & Technology Research Institute for Defence (STRIDE). It contains articles on research findings in various fields of defence science and technology. The primary purpose of this bulletin is to act as a channel for the publication of defence-based research work undertaken by researchers both within and outside the country.

WRITING FOR THE TECHNICAL DEFENCE S&T BULLETIN

Contributions to the journal should be based on original research in the areas related to defence science and technology. All contributions should be in English.

PUBLICATION

The editors' decision with regard to publication of any item is final. A paper is accepted on the understanding that it is an original piece of work which has not been accepted for publication elsewhere. Contributors will receive one complimentary copy of the issue in which their work appears.

PRESENTATIONS OF MANUSCRIPTS

The format of the manuscript is as below:-

a) MS Word format (preferably in Word 2007 format)
b) Single space.
c) Justified.
d) In Times New Roman 11-point font.
e) Should not exceed 15 pages, including references.
f) Margin should be 2 1/2 cm or 1 inch an all sides.
g) Texts in charts and tables should be in 10-point font.
h) Citations and references should follow the standard format.

Please e-mail the final paper to :

1) Dr. Zalini bt Yunus (yzalini@yahoo.co.uk)
2) Pn. Norkamizah bt Mohd. Nor (norkamizah@gmail.com)
3) Dinesh Sathyamoorthy (dinsat60@hotmail.com)

Template of the paper is as below

TITLE OF PAPER

Name of Author(s)

Address
Tel:
Fax:
E-mail:

Abstract

Contents of abstract.

Keywords: *Keyword 1; Keyword 2; Keyword 3.*

1. TOPIC

Paragraph 1.

Paragraph 2.

1.1 Sub Topic 1

Paragraph 1.

Paragraph 2.

2. TOPIC 2

Paragraph 1.

Paragraph 2.

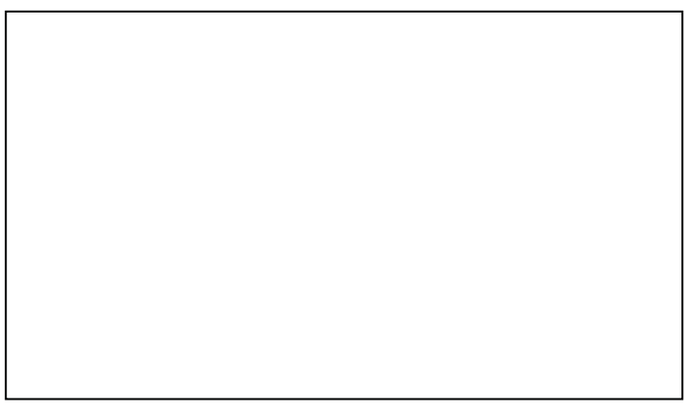

Figure 1: Title

Table 1: Title

Content	Content	Content
Content	Content	Content
Content	Content	Content
Content	Content	Content

Formula 1 (1)
Formula 2 (2)

REFERENCES

Long lists of notes of bibliographical references are generally not required. The method of citing references in the text is 'name date' sytle, e.g. 'Hanis (1993) claimed that...' or '…including the lack of interoperability (Bohara *et al*., 2003)'. End references should be in aplhabetical order.

1) Author(s) (Year). Title. Publisher, State Published.
2) Author(s) (Year). Title. Journal Title. Vol. , No. , pp. .
3) Website Title (Year). Website address. Accessed date and year.

THE EFFECT OF HEAT TREATMENT ON THE ELECTRICAL RESISTIVITY OF Al-5.5Zn-2.0Mg-2.0Sn ALLOY

Mahdi Che Isa*, Mohd Subhi Din Yati, Mohd Moesli Muhammad &
Nik Hassanudin Nik Yusoff

Maritime Technology Division,
Science & Technology Research Institute for Defence (STRIDE),
d/a KD MALAYA, Pangkalan TLDM, 32100 Lumut, Perak D.R.
Tel: 05-6817357
Fax: 05-6817350
Email: mahdicheisa@gmail.com

* Corresponding author

Abstract

Aluminium alloys with nominal composition of Al-5.5Zn-2.0Mg-2.0Sn (%wt.) have been fabricated by conventional casting technique under inert environment. Electrical properties, phase identification, microstructure and phase constituents of as-cast and heat treated alloy were studied by means of electrical resistivity measurement, X-ray diffractometry, confocal microscopy and energy dispersive x-ray. The results showed that Mg_2Sn intermetallic phase presence in both as-cast and heat treated alloy. The amount of Mg_2Sn phase presence in the heat treated alloy slightly decreased compared to as-cast condition. In addition, heat treatment was found to be able to improve microstructure as well as reduce electrical resistivity of the alloy.

Keywords: *Al-Zn-Mg-Sn alloys; Microstructure; Mhase characterisation; Heat treatment, Electrical resistivity.*

1. INTRODUCTION

Aluminium alloys have been developed in order to produce materials with improved properties for specific purposes. The excellent physical properties of aluminium alloys have made them attractive materials for various fields of application such as high strength structural materials, food containers, building, construction and etc. Heat treatment is often employed in practice in order to achieve ~~a~~ great improvement in physical properties (Berg *et al*., 2001; Cavazos *et al*., 2001; Werenskiold *et al*., 2000). Precipitation hardening improves physical and mechanical properties of the aluminium alloy, e.g. precipitate which can strengthen and act to impede dislocation motion through the materials (Gupta et al., 2001a; 2001b; Macchi *et al*., 2003). However, the magnitude of the precipitation effect can also influence other material properties such as electrical resistivity of the alloy. As it is well known that electrical resistivity has proved to be a powerful tool for investigating the physical changes in the heat treated aluminum alloys (Archambault & Dodard, 2000). Electrical resistivity measurements have often been used to study the precipitation process in precipitation hardening of aluminum alloys (Ferragut *et al*., 2002; Guyot & Cottignies, 1996). The aims of this study are to identify the phases present in the fabricated Al-Zn-Mg-Sn alloy and to investigate the effect of phase presence, microstructure and heat treatment on its electrical resistivity.

2. MATERIALS & METHODS

Aluminium alloy sample was prepared through a conventional casting technique under inert (argon) atmosphere. High purity metals (99.99%) of Al, Zn, Mg and Sn were mixed and melted in graphite crucible at 800ºC for 10 minutes and then poured into the steel mould to produce a casting of 18 mm in diameter and 12 cm in length. After casting process, part of the sample was cut and submitted to chemical analysis by atomic absorption spectrometer (Varian SpectraAA) following ASTM E 536-98 standard (ASTM E34 1985). The results are shown in Table 1. A fair agreement between nominal composition and the real one was established.

Table 1: Chemical composition of fabricated alloy

Composition							
Nominal (wt. %)				Chemical Analysis (wt. %)			
Al	Zn	Mg	Sn	Al	Zn	Mg	Sn
Bal	5.5	2.0	2.0	Bal	5.52	1.79	1.94

Bal: balance

Heat treated samples were homogenized at temperature 550 ºC for 24 hours and cooled in open air to room temperature (27ºC). Artificial ageing was carried out in an oven at temperature 150 ºC for 2, 3, 4, 5 and 6 hours. Three dimension (3D) confocal micrographs for as-cast and heat-treated samples were characterized by means of confocal laser scanning microscope and data analysis was done using the accompanied software (CLSM 5 Pascal) after the specimen was properly polished up to mirror quality. The phases present in the alloys were determined by X-ray diffractometer machine (Bruker AXS) with Cu Kα (λ = 1.543 Å) radiation source at scanning rate of 0.002 degrees per second with 2θ from 20º to 80º. The elements of the constituents phases were determined by scanning electron microscope (LEO VP 1430) complemented with energy dispersive X-ray systems (INCA). The conventional DC four point probe (Jandel, UK) was applied to measure the electrical resistivity where a current (100 µA) was passed through the sample during the measurement. Averages of 20 to 30 readings were reported in this study.

3. RESULTS & DISCUSSION

Figure 1 shows 3D confocal images of heat-treated and as-cast condition of Al-Zn-Mg-Sn alloys which consist of matrix α-Al, eutectic and black particles. The eutectic composition shows a slightly white colour and always following the contour of black particles. The obvious difference in morphology is the shape of black precipitate where the reticulate or long irregular shape turns into round shape and its size also became smaller after heat treatment was given. The homogenization process of polished surface of Al-Zn-Mg-Sn alloy mainly shows the spheroidisation phenomenon of irregular shape black particles. From the laser intensity profile for both alloys, it can be anticipated that it could have different phases due to interaction of different materials with laser beam during scanning process. To verify this, EDX analysis at the black spot was carried out and the elements present were Al, Mg, Zn and Sn as shown in Figure 2. It is strongly believed that black precipitates are new phases or intermetallics of the above elements. Since tin has a very low solid solubility limit in aluminium at room and high temperature, it will be rejected from the matrix to grain boundary during the solidification process and it has a very high tendency to act as nuclei to form new intermetallic phases. The strong Al peak in the EDX spectrum is believed to be from the aluminium matrix as a result of the X-ray beams being bigger than the precipitates, thus enabling aluminium to be detected during analysis.

The X-ray diffraction spectrum of treated and untreated alloys is shown in Figure 3. Further investigation and phase identification showed that the positions of diffraction peaks are almost similar for heat treated and as-cast alloy. The XRD pattern confirmed that a new phase belongs to Mg_2Sn intermetallics compound with lattice parameter value of 0.676 nm (JCPDS card number 7-274). The Mg_2Sn crystallizes in the antifluorite cubic structure under normal conditions of pressure and temperature as the equilibrium structure is present in both treated and untreated alloys (Masaki *et al*., 1990; Urretavizcaya & Meyer, 2002). Therefore it can be concluded that this alloy consists of two phases which are black particles which is Mg_2Sn intermetallics and white which is α-Al as depicted in Figure 1. Other phases are not presence because both Mg and Zn have high solid solubility in aluminium. The shapes of these particles depend on heat treatment and it was seen that the intermetallic phases in as-cast alloy are bigger in size compared to the heat treated sample. The intensity of XRD peaks for Mg_2Sn in the heat treated alloy shows a decrease in the peak intensity compared to as-cast alloy. This phenomenon can be attributed to the dissolution process of Mg_2Sn intermetallics into solute atoms of Mg and Sn or oxides of Mg and Sn during homogenization in air which in turn reduces the presence amount of Mg_2Sn phase. At this point, we found that homogenization is capable of increasing or enriching with solute atoms in the aluminium matrix and it is expected to improve other physical properties.

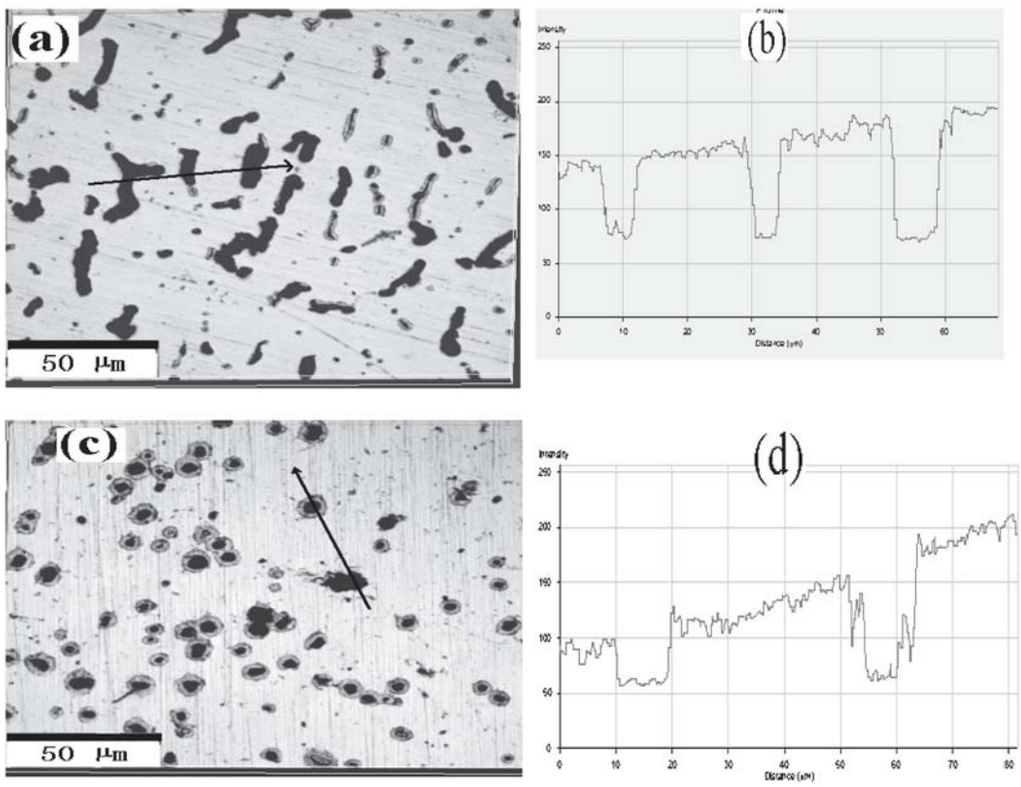

Figure 1: 3D Confocal micrograph of Al-Zn-Mg-Sn alloy (a) As-cast with the indicated box has a dimension of 180 x 180 x 20 µm (b) Laser intensity profile for as-cast sample in the region as marked by arrow (c) Heat treated with the indicated box has a dimension of 180 x 180 x 15 µm (d) Laser intensity profile for heat treated sample in the region as marked by arrow.

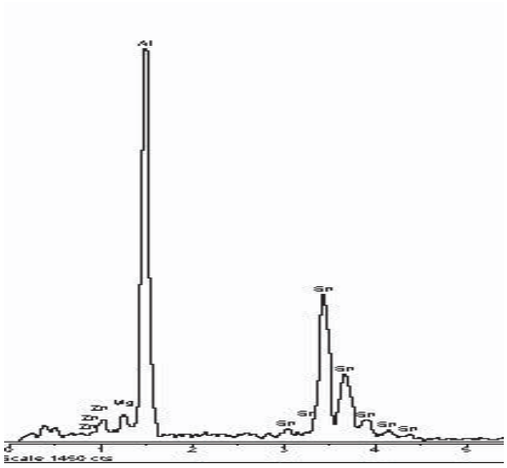

Figure 2: EDX microanalysis on the black precipitates of Al-Zn-Mg-Sn alloy.

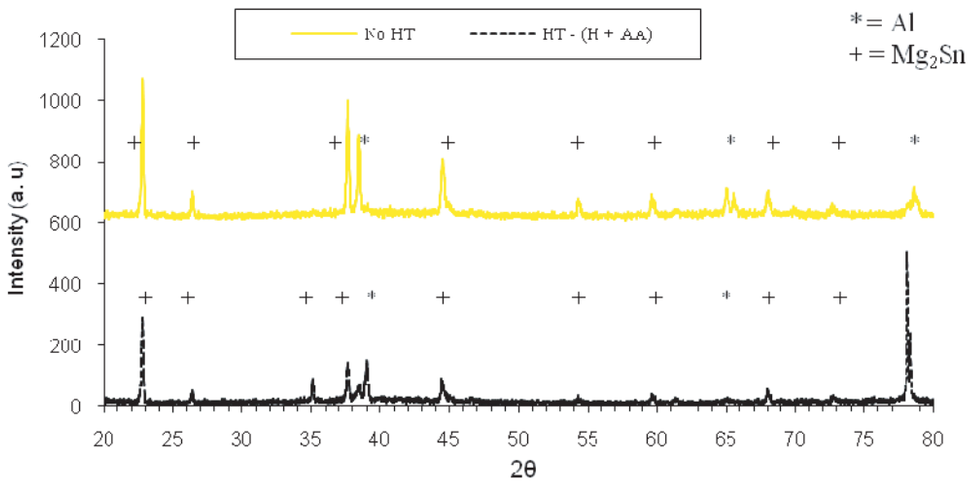

Figure 3: XRD pattern for as-cast and heat treated Al-Zn-Mg-Sn alloy
HT = Heat treatment, H = Homogenizing, AA = Artificial ageing.

Figure 4 shows the value of electrical resistivity as a function of ageing time at 150ºC after homogenization. The electrical resistivity for ageing time that equals to zero is that of the as-cast sample. Electrical resistivity for the as-cast sample decreases from 36.44 μΩ.mm to 33.33 μΩ.mm after homogenization and artificial ageing for two hours. High electrical resistivity in the as-cast sample may be contributed by the scattering of electron through various shape grains and precipitate arrangement in dendrite structure. Other metallurgical factors and microstructure defect such as voids, microporosity, dislocation density, intermetallics, fine or coarse precipitates and grain shape also can influence electron mobility in the alloy (Schaffer *et al*., 1999). The decrease in electrical resistivity after the homogenization

process can be explained by the improvement of microstructural factors such as less vacancy concentration, more solute atoms concentration in the matrix, smaller precipitate size and precipitate volume fraction (Archambault & Dodard, 2000; Guyot & Cottignies, 1996). For a longer ageing time, the electrical resistivity values have slightly increased and maintained, but it was still low compared to the as-cast sample. When the ageing time proceeds, the increase of resistivity was observed as a result of more precipitates formed and as well as the increase in the electron scattering effect as already shown by Guyot & Cottignies (1996).

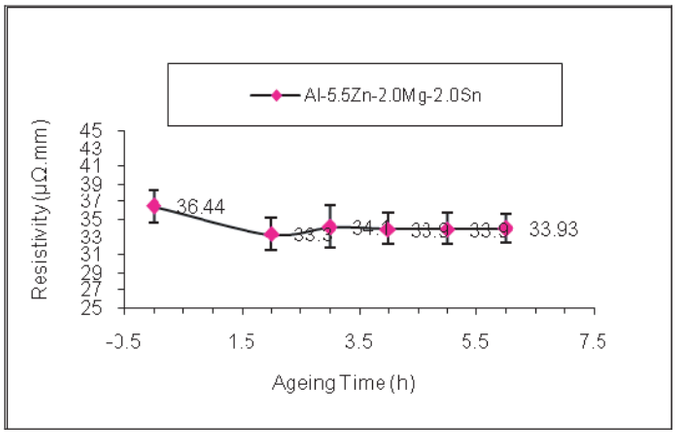

Figure 4: Electrical resistivity values as a function of ageing time at 150ºC after homogenizing at 550ºC for 24 hours.

4. CONCLUSION

In conclusion, we found that the microstructure was altered with the heat treatment and it was observed that the irregular shape reticule black particles change into round shape and dispersed evenly in the alloys. Heat treatment has been proven to reduce the electrical resistivity of Al-Zn-Mg-Sn alloy by dissolving intermetallic phases to solute atoms, improve the microstructure of the grains as well as modifying the shape of precipitate. This will reduce or eliminate microstructure defects and electron scattering effects in the alloy by maximizing electron mobility and thus reducing electrical resistivity.

ACKNOWLEDGEMENTS

The authors wish to thank and acknowledge the Government of Malaysia for supporting and funding this project.

REFERENCES

ASTM E34. (1985). Standards Test Methods for Chemical Analysis of Aluminum and Aluminum Alloys, American Society for Testing and Materials, Philadelphia.

Archambault, P. & Dodard, D. (2000). High temperature precipitation kinetics and ttt curve of a 7xxx alloy by in-situ electrical resistivity measurements and differential calorimetry. *Scripta Materilia*, **42**: 675.

Berg, L.K., Gjønnes, J., Hansen, V., Li, X.Z., Knutson-Wedel, M., Waterloo, G., Schryvers, D. & Wallenberg, L.R. (2001). GP-zones in Al–Zn–Mg alloys and their role in artificial aging. *Acta Materialia*, **49:** 3443-3451.

Cavazos, J.L. & Colás, R. (2001). Precipitation in a heat-treatable aluminum alloy cooled at different rates. *Materials Characterization*, **47:** 175-179.

Ferragut, R., Somoza, A. & Torriani, I. (2002). Pre-precipitation study in the 7012 Al-Zn-Mg-Cu alloy by electrical resistivity. *Materials Sci. Eng.*, **A 334:** 1-5.

Gupta, A.K., Lloyd, D.J. & Court, S.A. (2001a). Precipitation hardening in Al-Mg-Si alloys with and without excess Si. *Materials Sci. Eng.*, **A 316:** 11-17.

Gupta, A.K., Lloyd, D.J. & Court, S.A. (2001b). Precipitation hardening processes in an Al-0.4%Mg-1.3%Si-0.25%Fe aluminum alloy. *Materials Sci. Eng.*, **A 301:** 40-146.

Guyot, P. & Cottignies, L. (1996). Precipitation kinetics, mechanical strength and electrical conductivity of AlZnMgCu alloys. *Acta Materialia*, **44**: 4161-4167.

Macchi, C. E., Somoza, A., Dupasquier, A. & Polmear I. J. (2003). Secondary precipitation in Al–Zn–Mg–(Ag) alloys. *Acta Materialia*, **51**: 5151-5158.

Masaki, T., Okamoto, H., Subramaniam, P. & Kacprzak, L. (Eds). (1990). Binary Alloys Phase Diagrams, 2nd Edition, American Society for Metals, Metals Park, OH.

Schaffer, P., Saxena, A., Antolovich, S.D., Sanders, T.H. & Warner, S.B. (1999). The Science and Design of Engineering Materials, 2nd Edition, McGraw Hill International. Singapore.

Urretavizcaya, G. & Meyer, G.O. (2002). Metastable hexagonal Mg_2Sn obtained by mechanical alloying. *J. Alloys & Compounds*, **339**: 211-215.

Werenskiold, J.C., Deschamps, A. & Bréchet, Y. (2000). Characterization and modeling of precipitation kinetics in an Al-Zn-Mg alloy. *Materials Sci. Eng.*, **A 293**: 267-274.

WHOLE BODY VIBRATION (WBV) ON MALAYSIAN ARMED FORCES (MAF) VEHICLES

Shamsul Akmar Ab Aziz*, Adam Hj Gani & Abdul Hamid Hassan

Mechanical & Aerospace Technology Division,
Science & Technology Research Institute for Defence (STRIDE),
Taman Bukit Mewah Fasa 9, 43000 Kajang, Selangor D.E.
Tel: 03-87324510
Fax: 03-87336219
E-mail: saaa.pst@mod.gov.my

***** Corresponding author

Abstract

Health Hazard Assessment (HHA) was performed by the Vehicle Branch, Science & Technology Research Institute for Defence (STRIDE), to evaluate the Whole-Body Vibration (WBV) health hazards of MAF vehicles. The analysis is performed based on the measurements taken in the Land Rover Defender Puma, Tracked Load Carrier (TLC) Doosan and 3-Ton Truck Mercedes Benz. In addition, this paper also describes the new measurement method employed, and highlight the comparative study of the health risk prediction using the current whole-body vibration (WBV) International Organizational Standard (ISO 2631-1) Evaluation of human exposure to whole-body vibration – Part 1: General requirements.

Keywords: *Whole Body Vibration (WBV); Malaysian Armed Forces (MAF) Vehicles; Vibration Exposure; Health Hazard Assessment (HHA); Comfort Reactions.*

1. INTRODUCTION

Operating vehicles and machinery expose humans to mechanical vibrations which can interfere with comfort, working efficiency and in some circumstances, health and safety. Vehicle movement causes mechanical energy in the form of vibration to propagate throughout the vehicle's structure. There are two types of occupational vibration; hand arm vibration (HAV) and whole body vibration (WBV). HAV is transmitted through the hands and arms, and is known to cause specific health effects such as Raynaud's syndrome (Ohcow Office, 2005). WBV is transmitted through the body's supporting surfaces such as the legs when standing and the back and buttocks when sitting. In military operation perspective, this vibration, can affect the health and readiness of the soldiers. The relevant literatures of the effects of long-term high-intensity WBV indicate an increased health risk to the lumbar spine and the connected nervous system of the segments affected.

This study is a continuation of an ongoing research focusing on the effects of dynamic ride environment on the performance of seated in-vehicle reaching tasks, especially on occupants of off-road vehicles who are regularly exposed to WBV that impairs their ability to perform fast and precise in-vehicle tasking while the vehicle is in motion.

The total vibration levels in the z-axis (buttocks-to-head for a seated person) were assessed according to a previous version of the International Standard for evaluation of human exposure to whole-body vibration (ISO 2631-1, 1997), which defined exposure limits, reduced comfort boundaries and fatigue-decreased proficiency boundaries. The objective of the study was to characterize the vibration levels at different positions inside several MAF vehicles. Comparison of the vibration levels with existing standards will enable the development of guidelines for safe vibration exposure, thus making a significant impact on improving the health and safety of MAF personnel. This paper will characterize and quantify the nature of

this performance degradation, while aiding the development of dynamic models as well as design standards and strategies for reducing WBV-related errors in performance. Our research will enable these errors to be mitigated through improved design of controls, displays, vehicle suspension, and seating systems.

2. ASSESSMENT OF WHOLE-BODY VIBRATION EXPOSURE

ISO 2631 defines and gives numerical values for limits of exposure for vibrations transmitted from solid surfaces to the human body in the frequency range of 1 to 80 Hz. These limits are given for use according to the three generally recognisable criteria of preserving comfort, working efficiency and safety or health. The limits are as follows (Fostrer *et al*., 2001):

i. Exposure limits – is related to preserving health and safety and set half of the threshold of pain.
ii. Fatigue decreased proficiency boundary – is concerned with the preservation of working efficiency said to define a limit beyond which exposure to vibration might impair working efficiency for many of tasks, particularly those in which time dependent effects such as fatigue are known to worsen performance.
iii. Reduced comfort boundary – is concerned with the preservation of comfort and based on studies in transport industry.

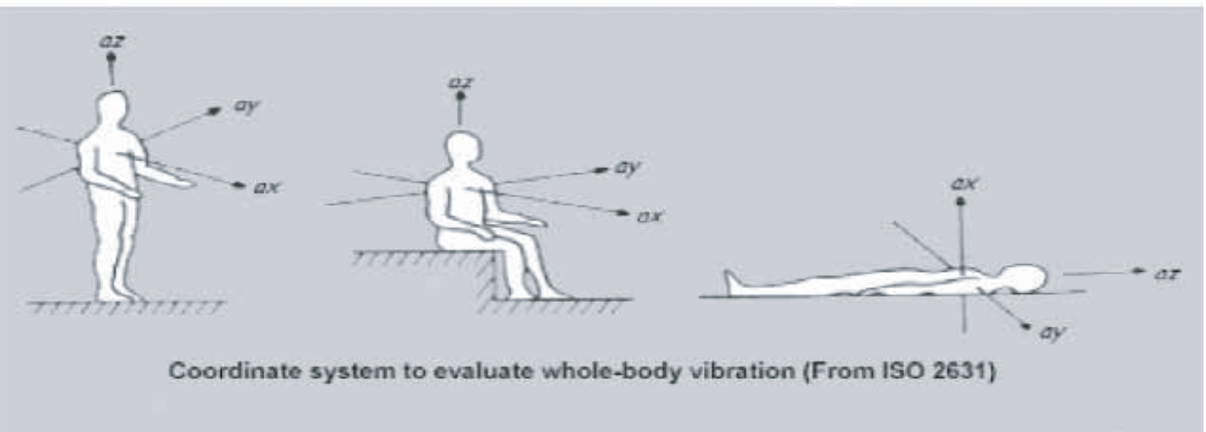

Figure 1: Coordinate system to evaluate whole-body vibration (Source: ISO 2631-1 (1997))

Different weightings based on human body sensitivity are applied to vertical and horizontal vibrations (Figure 1). The vertical vibration (z-axis) criteria curve has its highest sensitivity between 4- 8 Hz while horizontal vibration (x and y axes) is in between 1-2 Hz. With respect to the "fatigue-decreased proficiency", the reference curves for "exposure limits" are 6 dB (acceleration times 2) higher and the reference curves for "reduced comfort" are 10 dB (acceleration divided by 3.15) lower.

Figure 2 shows the "fatigue-decreased proficiency" reference curves for vibration along the x and y axes (i.e. lateral vibration).

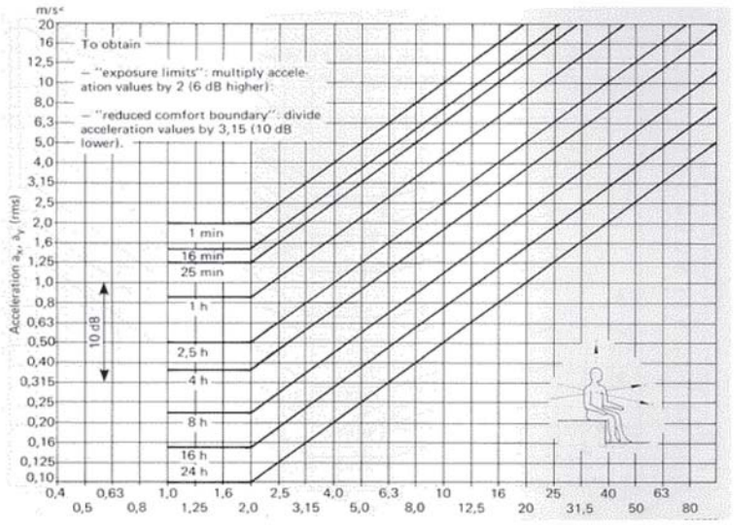

Figure 2: Fatigue decreased proficiency references curves (Source: ISO 2631-1 (1997)).

Figure 3 shows the "fatigue-decreased proficiency" reference curves for vibration along the z axis (head to toe). In this chart, the rms acceleration has been plotted (like octave-band L_p on a Noise Rating Chart).

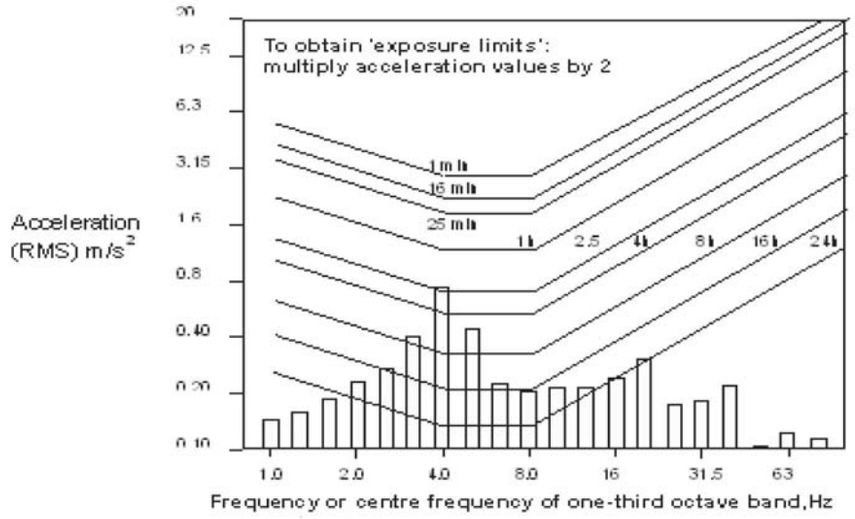

Figure 3: Frequency of centre frequency of one-third octave band (Source: ISO 2631-1 (1997)).

ISO 2361-1 (1997) does not give specific limits of vibration magnitude as related to comfort due to the many factors which vary with each type of environment and application. The standard however does provide values which gave an approximate indication of likely reactions from exposed drivers to various

magnitudes of overall vibration values. Table 1 shows the "Comfort reactions to vibration environments" (ISO 2631-1, 1997).

Table 1: Comfort reactions to vibration environments (Source: ISO 2631-1 (1997)).

Vibration Value (m/s^2)	Comfort reactions
< 0.315	Comfortable
0.315 - 0.63	A little uncomfortable
0.5 – 1.0	Fairly uncomfortable
0.8 – 1.6	Uncomfortable
1.25 – 2.5	Very uncomfortable
>2.5	Extremely uncomfortable

ISO 2631-1 (1997) makes allowance for health guidance caution zones, which allows the application of a rough assessment of likely health effects taking into account the vibration (rms) values and exposure periods (Figure 4). However, the standard does not offer a definite means for predicting such effects. For exposures below the zone, the ISO 2631-1 (1997) standard warns that health effects have not been clearly documented and/or objectively observed. Caution with respect to potential health effects is therefore indicated, while above the zone, health risks are likely (Joubert, 2002).

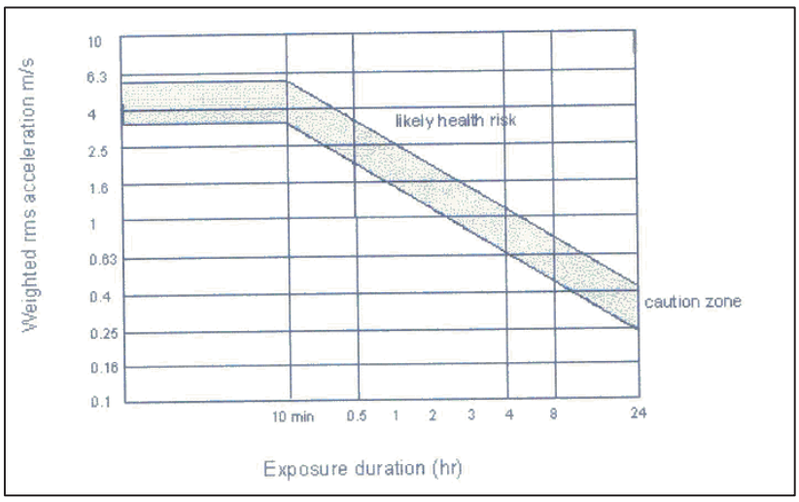

Figure 4: Health guidance zone (Source: ISO 2631:1 (1997)).

3. METHODOLOGY

3.1 Types of Vehicles

Three types of vehicles were used in this study: Land Rover Defender Puma, Tracked Load Carrier (TLC) Doosan and 3-Ton Truck Mercedes Benz. The Land Rover Defender Puma and 3-Ton Truck Mercedes Benz are wheeled vehicles, while the Tracked Load Carrier (TLC) is a tracked vehicle.

3.2 Methods

WBV of seated person was measured using a seat pad containing 3 accelerometers (vibration transducers). The accelerometers measured the vibration in the x- (fore-to-aft), y- (left-to-right side) and z- (buttocks-to-head) axes. The army personal will sit on the triaxial seat transducer that was aligned on the seat. The vehicle vibration will be transmitted to the body through triaxial transducer. The triaxial transducer was connected to a 3-Channel Human Vibration Front-end Bruel & Kjaer Type 1700 or Human Vibration Type 4447, which logged the total vibration levels in each axis in units of meters per second squared (m/s^2). The measurements were carried out in four conditions; at idle, and at velocities of 20km/h, 40km/h and 60km/h. The vehicle's speed has to be stable for a few minutes at every condition while the pavement road condition has to be straight for at least 3 km.

For all vehicles, triaxial accelerometers were placed on the driver, co-driver and passenger positions. The MAF personnel were seated facing sideways in the vehicle. Each personnel was measured with a triaxial accelerometer that was mounted on the frame of the seat.

4. RESULTS & DISCUSSION

4.1 Land Rover Defender Puma (Figure 5)

This trial was carried out by the STRIDE team on Jun 2008, at Air Strip Kahang, Johor (STRIDE, 2008). The road is of pavement type, and the measurements were taken for the driver, co-driver and passenger positions at various velocities (Table 2).

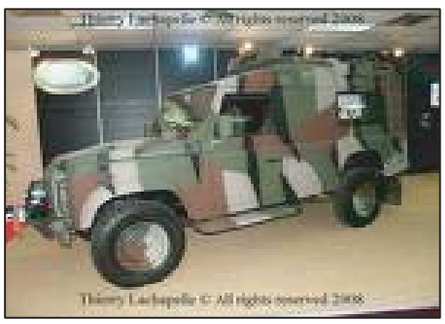

Figure 5: **Land Rover Defender Puma.**

Table 2: **Land Rover Defender Puma WBV Data.**

Measurement Seat	Velocity (km/h)	RMS acceleration (m/s^2)				Exposure Limit (hour)	Comfort Reactions
		x-axis	y-axis	z-axis	Vibration Total Value (VTV)		
Driver	Idle	0.000	0.000	0.018	0.018	>8	Comfortable
	20	0.071	0.085	0.147	0.214	5	Comfortable
	40	0.124	0.109	0.274	0.361	2.5	A little uncomfortable
	60	0.225	0.145	0.449	0.588	1.5	A little uncomfortable
	80	0.149	0.106	0.246	0.356	3.0	A little uncomfortable
	90	0.140	0.086	0.252	0.342	2.0	A little uncomfortable
	110	0.162	0.093	0.281	0.385	0.5	A little uncomfortable
Co-driver	Idle	0.000	0.023	0.029	0.044	>8	Comfortable
	20	0.077	0.079	0.161	0.224	5	Comfortable
	40	0.166	0.133	0.230	0.426	2.3	A little uncomfortable
	60	0.170	0.147	0.383	0.499	1.5	A little uncomfortable
Passenger	Idle	0.036	0.000	0.030	0.060	>8	Comfortable
	20	0.120	0.069	0.223	0.296	4.5	Comfortable
	40	0.172	0.132	0.349	0.468	1.6	A little uncomfortable
	60	0.212	0.127	0.668	0.754	1.0	Fairly uncomfortable

The vibration values, exposure limit and comfort reactions for the Land Rover Defender Puma are shown in Table 2. The measurements were carried out for the driver, co-driver and passenger positions for each of the four conditions; idle, 20km/h, 40km/h and 60km/h. Other additional conditions were at 80km/h, 90km/h and 110km/h for the driver position only. The highest total vibration level of 0.754 m/s^2 was observed at 60km/h for the passenger position. At 60km/h, the vibration total value (VTV) for passenger position is higher than the driver and co-driver positions. The vibration increased with increasing velocity. Comparison between vibration values with comfort reactions to vibration environment (Table 1) shows that the passenger was fairly uncomfortable at these vibration values.

4.2 Tracked Load Carrier (TLC) Doosan (Figure 6)

The trial was carried out by the STRIDE team on August 2005, at Kem Gemas, Negeri Sembilan (Figure 7). The road is of pavement type, and the measurements were taken for driver and co-driver positions (STRIDE, 2005a).

Figure 6: TLC Doosan.

Figure 7: Measuring WBV on TLC.

Table 3: **Tracked Load Carrier (TLC) Doosan WBV Data.**

Measurement Seat	Velocity (km/h)	Vibration Total Value (VTV)	Exposure Limit (hour)	Comfort Reactions
Driver	Idle	0.035	>8	Comfortable
	20	0.474	1.5	A little uncomfortable
	30	0.689	0.9	fairly uncomfortable
	50	0.609	1.3	fairly uncomfortable
Co-driver	Idle	0.031	>8	Comfortable
	20	0.373	2.5	A little uncomfortable
	30	0.407	2	A little uncomfortable
	50	0.581	1.4	fairly uncomfortable

The vibration levels, exposure limit and comfort reactions for different driving velocities are shown in Table 3. As shown, the vibration values at the driver position were higher than at the co-driver position. The highest level of vibration was experienced when the vehicle was driven at a velocity of 50 km/h of which the vibration value was 0.609 m/s^2 and exposure limit was 1.3 hours at the driver position. At the same speed, the vibration value at the co-driver position was 0.581 m/s^2 and exposure limit was 1.4 hours.

4.3 3-Ton Truck Mercedes Benz 4X4 911B/911C (Figure 8)

This trial was carried out by the STRIDE team on Jun 2005 **(**STRIDE, 2005b**).** The road is of pavement type, and the measurements were taken at four conditions; idle, 20km/h, 40km/h and 60km/h. The WBV test data were taken at the driver and co-driver positions.

Figure 8: 3-Ton Truck Mercedes Benz.

Table 4: **3-Ton Mercedes Benz 4X4 911B/911C WBV Data.**

Measurement Seat	Velocity (km/h)	Vibration Total Value (VTV)	Exposure Limit (hour)	Comfort Reactions
Driver	Idling	0.10	>8	Comfortable
	20	0.49	1.0	A little uncomfortable
	40	0.65	0.9	Fairly uncomfortable
	60	0.64	1.1	Fairly uncomfortable
Co-driver	Idling	0.24	5	Comfortable
	20	0.49	1.5	A little uncomfortable
	40	0.58	1.4	Fairly uncomfortable
	60	0.74	0.7	Fairly uncomfortable

The vibration values for different driving velocities are shown in Table 4. The vibration increased with increasing velocity. The highest level of vibration of 0.74 m/s^2 was experienced at the co-driver position, when the vehicle was driven at a velocity of 60 km/h of which the co-driver will be fairly uncomfortable.

5. CONCLUSION

The dominant driver seat WBV component is along the z-axis vertical direction. The vibration levels and dose values for Land Rover Defender Puma, Tracked Load Carrier (TLC) and 3-Ton Truck Mercedes Benz were evaluated according to the ISO standards. The vibration exposure was depended on the type of terrain and the vehicle velocity, factors that are unlikely to be controlled in practice. Therefore, it is recommended that seatbelts be worn when available. This study also provided information about the WBV spectra for three vehicles, which was not previously available. This data is useful in the design of future studies on the effects of vibration on performance.

6. SUGGESTIONS

Minimizing the vibration exposure of MAF personnel is important to reduce the injury risks associated with vibrating equipment and hand tools, as well as maximizing productivity. The vibration values on MAF vehicles can be reduced by:

i. Improving vehicle suspension
ii. Altering the position of the seat within the vehicle
iii. Mounting equipment on springs or compression pads
iv. Maintaining equipment properly (e.g., balance and replace worn parts)
v. Modifying the seat and control positions to reduce the incidence of forward or sideways leaning of the trunk, and provide back rest support
vi. Using materials that generate less vibration
vii. In seated tasks; providing a spring or cushion as a vibration isolator
viii. In standing operations; providing a rubber or vinyl floor mat
ix. Reducing the speed of travel
x. Minimizing the exposure period by alternating working tasks where vibration is present
xi. Increasing rest/recovery time between exposures.

ACKNOWLEDGEMENTS

The Authors would Dr. Zalini binti Yunus, Head of the Human Factor Branch, for her valuable advice and support in preparing this paper.

REFERENCES

Abel, S.M., Borland, M.J. & Nakashima, A.M. (2005). Characterization of Noise and Vibration Exposures in Canadian Forces Land Vehicles. Defence R&D, Canada, Toronto.

Fostrer, G., Mabbott, N. & McPhee, B. (2001). Heavy Vehicle Seat Vibration and Driver Fatigue. Australian Transport Safety Bureau.

ISO 2631-1 (1997). Evaluation of human exposure to whole-body vibration – Part 1: General requirements.

Joubert., D.M. (2002). Whole Body Vibration in Developing Country, a pilot study in South Africa amongst forklift driver at the port of Durban.

Ohcow Office (2005). Whole body vibration. Occupational health clinics for Ontario Workers.

STRIDE (2005a). Laporan STRIDE Ujinilai Kenderaan 'Tracked Load Carrier' TLC Keluaran Syarikat Doosan Infracore Co. Ltd, Korea Selatan.

STRIDE (2005b). Laporan STRIDE Ujinilai 'Technology Demonstrator' Trak 3 Ton Mercedes Benz 4X4 911B/911C yang telah di Baikpulih.

STRIDE (2008). Laporan STRIDE Ujinilai Kenderaan Land Rover Defender Puma 4X4 untuk Kegunaan Tentera Darat.

HEAT STRESS IN VARIOUS **TYPES OF MILITARY VEHICLES IN MALAYSIAN (TROPICAL) CLIMATE**

Adam bin Hj Gani*, Shamsul Akmar Ab Aziz & Abdul Hamid Hassan

Technology and Aerospace Division,
Science & Technology Research Institute for Defence (STRIDE),
Taman Bukit Mewah, Fasa 9, 43000 Kajang, Selangor D.E.
Tel: 0387324510
Fax: 0387336219
Email: ag_stride@yahoo.com

* Corresponding author

Abstract

The effect of heat stress on the Malaysian Armed Forces (MAF) in Malaysian climate is very important to be determined. The work areas (inside the vehicle) in which MAF personnel are exposed to is a crucial parameter to be monitored. The hot weather in Malaysia may cause heat disorders such as heat stroke, heat exhaustion, heat cramps, heat fainting and heat rashes. Environmental heat load can be modified by engineering controls such as ventilation, air conditioning, screening, insulation, and modification of process or operation. In Malaysia, the temperature can reach up to 40 ^{o}C on sunny days. Hence, it is compulsory to provide each MAF vehicle with an air conditioning system. Failure to do so will cause serious health problems to MAF personnel. In order to measure the heat stress, the wet bulb globe temperature (WBGT) index is used. To perform the measurements, equipments such as INNOVA 1221 Thermal Comfort Data Logger and 7301 Application software, black globe bulb thermometer, natural wet bulb thermometer and dry bulb thermometer are used.

Keywords: *Heat Stress; Wet bulb globe temperature (WBGT); Malaysian climate.*

1. INTRODUCTION

This study is aimed at determining the effect of tropical climate specifically on heat stress on the Malaysian Armed Forces (MAF) personnel operating inside various types of military vehicles. Heat stress is defined as the effect on a person exposed to a hot environment and the characteristics of the environment governing heat transfer between the atmosphere and the body. The total heat stress is considered to be the sum of heat generated in the body (metabolic heat) plus the heat gained from the environment (environmental heat) minus the heat lost from the body to the environment. The bodily response to total heat stress is called the heat strain (ISO 7243, 1982).

The vehicles design, materials and air-conditioning systems are closely monitored. The wet bulb globe temperature (WBGT) index is one of the empirical indices representing the heat stress which an individual is exposed to. The factors of air temperature, relative humidity of air, the presence of hot or cold objects in the surrounding area and the presence of air movement shall be taken into account.

1.1 The Body Reaction to Heat Stress

For this study, we focus on the Malaysian military vehicle interior space as a work area. Individual factors such as age, weight, fitness, medical condition and acclimatization to the heat may contribute to heat stress.

When the body is exposed to external heat, the body system will circulate blood to the skin, which increases skin temperature and allows the body to give off its excess heat through the skin (Null, 2003). However, if the muscles are being used for physical labor, less blood is available to flow to the skin and release the heat. Sweating is another means the body uses to maintain a stable internal body temperature in the face of heat. However, sweating is effective only if the humidity levels is low enough to permit evaporation and if the fluids and salts lost are adequately replaced.

The level of heat stress at which excessive heat strain will result depends on the heat-tolerance capabilities of the worker. If the body cannot dispose of excess heat, the body's core temperature rises and the heart rate increases. As the body continues to store heat, the individual begins to lose concentration and has difficulty focusing on a task, may become irritable or sick, and often loses the desire to drink. The next stage is most often fainting, and death is possible if the person is not removed from the heat stress.

Many of the bodily responses to heat exposure are desirable and beneficial. However, at some level of heat stress, the worker's compensatory mechanisms will no longer be capable of maintaining body temperature at the level required for normal body functions. As a result, the risk of heat-induced illnesses, disorders and accidents substantially increases. In order to reduce excess heat the person has to move to a cooler place, reduce the work space or load, or remove or lose some clothing (NIOSH, 1986).

2. ENVIRONMENTAL FACTORS

Four environmental factors that affect the amount of stress a worker faces in a hot work area are dry bulb (air) temperature, humidity, radiant heat (such as from the sun or a furnace) and air velocity. Assessment of heat stress may be conducted by measuring the climatic and physical factors of the environment and then evaluating their effects on the human body by using an appropriate heat stress index (NIOSH, 1986).

2.1 Dry Bulb (Air) Temperature (t_a)

The dry bulb temperature is the simplest to measure of the heat stress. It is the temperature of the ambient air as measured with a thermometer. Temperature units proposed by the International Standards Organization (ISO) are degrees Celsius (or Centigrade) C= (^{o} F -32) x 5/9 and degrees Kelvin $^oK = {}^oC + 273$ (NIOSH, 1986).

The general precautions which must be considered when using any thermometer are as follows:

i. The temperature to be measured must be within the measuring range of the thermometer.
ii. The time allowed for measurement must be greater than the time required for thermometer stabilization.
iii. The sensing element must be in contact with or as close as possible to the area of thermal interest.
iv. Under radiant conditions (e.g. in sunlight or where the temperature of the surrounding surfaces is different from the air temperature) the sensing element should be shielded.

2.2 Humidity

Humidity, the amount of water vapor within a given space, is commonly measured as relative humidity. The higher the water vapor pressure, the lower will be the evaporative heat loss. The natural wet bulb temperature (t_{nwb}) is the temperature measured by a thermometer which has its sensor covered by wetted cotton wick and exposed only to the natural prevailing air movement. Accurate measurements of t_{nwb} require using a clean wick, distilled water and proper shielding to prevent radiant heat gain (NIOSH, 1986).

2.3 Air Velocity

Wind, whether generated by body movements or air movement (V_a), is the rate in feet per minute (fpm) or meters per second (m/sec) at which the air moves and is important in heat exchange between the human body and the environment, because of its role in convective and evaporative heat transfer. Wind velocity is measured with an anemometer (NIOSH, 1986).

2.4 Radiation

Radiant heat sources can be classified as artificial (e.g. infrared radiation in such industries as iron and steel industry, the glass industry, foundries) or natural such as solar radiation. Black Globe Thermometer was developed to measure radiant heat. The thermometer consists of a 15 centimeter hollow copper sphere (a globe) painted a matte black to absorb the incident infrared radiation and a sensor (thermocouple) with its sensing element placed in the center of the globe. Black globe thermometers exchange heat with the environment by radiation and convection. The temperature stabilizes when the heat exchange by radiation is equivalent to the heat exchange by convection (NIOSH, 1986).

3. OBJECTIVES

This study was requested by the MAF to fulfill the requirements of military standards. The pervasive problem in military vehicles is the need to extend the useful life of human body system. The increase in body temperature due to heat will affect safety and health, and reduce the military personnel performance. The objectives of this project are as follows:

i. To ensure the imported military vehicles are safe and comfortable for the military personnel.
ii. To ensure the design of military vehicles are suitable for the Malaysia climate.
iii. To increase awareness of the heat stress effects.
iv. To show a method to perform Heat Stress test in Malaysian climate.

By presenting this paper, it is with hope that the ideas and methods will be applied in all military vehicles.

4. METHODS

The Wet Bulb Globe Temperature (WBGT) index is a basis for environmental heat stress monitoring to control heat casualties at military camps. The advantages are the measurements are few and easy to conduct. For indoor use, only two measurements are needed, natural wet bulb and black globe temperature. For outdoors in sunshine, the air temperature must also be measured. The wet bulb globe temperature (WBGT) is calculated by using the following equations (ISO 7243, 1982):

- For indoors or outdoors without direct sun exposure:

$$WBGT = 0.7t_{nwb} + 0.3t_g \quad (1)$$

- For outdoors with direct sun exposure:

$$WBGT = 0.7t_{nwb} + 0.2t_g + 0.1t_a \quad (2)$$

WBGT = Wet Bulb Globe Temperature
t_{nwb} = Natural Wet Bulb Temperature
t_g = Black Globe Temperature
t_a = Air Temperature

4.1 Equipments

The determination of WBGT requires the use of the following apparatus (Figure 1):

i. INNOVA 1221 Thermal Comfort Data Logger and 7301 Application software.
ii. Black globe bulb thermometer (-5^{o}C to +100^{o}C with accuracy of $\pm$ 0.5^{o}C)
iii. Natural wet bulb thermometer (-5^{o}C to +50^{o}C)
iv. Dry bulb thermometer
v. Distilled water.

Figure 1: Heat Stress Equipment consist of Black globe bulb thermometer, natural wet bulb thermometer and dry bulb thermometer.

4.2 Preparation

Before the measurement, the following conditions must be met:

i. The dry bulb thermometer must be shielded from the sun and the other radiant surfaces of the environment without restricting the air flow around the bulb.
ii. The wick of the natural wet bulb thermometer should be kept wet with distilled water for at least half an hour before the temperature reading is made. The wick must be wet by direct application of water from a syringe half an hour before reading. The wick should always be clean, and new wicks should be washed before using.
iii. A globe thermometer, consisting of a 15 cm in diameter hollow copper sphere painted on the outside with a matte black finish, or equivalent, must be used. The globe should be exposed at least 25 minutes before it is read.
iv. A stand should be used to suspend the three thermometers so that they do not restrict free air flow around the bulbs, and the wet-bulb and globe thermometer are not to be shaded.

4.3 Methods

Environmental heat exposure shall be assessed by the Wet Bulb Globe Thermometer (WBGT) method or equivalent techniques, such as Effective Temperature (ET), Corrected Effective Temperature (CET), or Wet Globe Temperature (WGT) that can be converted to WBGT values (ISO 7243, 1982). To perform the heat stress measurement inside the vehicle, the following conditions must be followed:

i. Temperature rise was measured continuously over two hours in sunny days with ambient temperatures ranging from 30 to 35^{o}C.
ii. Temperature is recorded continuously every 5 minutes under direct sunlight.
iii. Air-conditioning shall be in maximum capacity and all doors are closed to ensure the internal temperature of the vehicle is at the coolest temperature possible.
iv. If there is no air conditioning system equipped, all windows must be opened.
v. The equipment shall be set up at least half an hour before measurements are taken.

4.4 Types of Vehicles to be Tested

i Main Battle Tank PT91 (Figure 2)

Figure 2: Main Battle Tank PT-91

ii Track Load Carrier (TLC) (Without Air Conditioning System) (Figure 3)

Figure 3: Track Load Carrier

iii VAMTAC 4x4 (Without Air Conditioning System) (Figure 4)

Figure 4: Vamtac 4x4

iv Tatra 7 Ton (Figure 5)

Figure 5: Tatra 7 Ton

v Tatra 10 Ton (Figure 6)

Figure 6: Tatra 10 Ton

4.5 Data Collection

Internal temperature of military vehicles was recorded continuously with INNOVA 1221 Thermal Comfort Data Logger complete with the sensors mentioned above. Temperature sensors were placed in the test vehicles at the rear passenger cabin. The sensors were placed in shaded areas and not in direct contact with any part of the vehicle. All data were transmitted and saved automatically to the installed software.

4.6 Statistical Analysis

The data were recorded on an excel spreadsheet for statistical analysis. The graphs of WBGT (^{o}C) versus time (t) were plotted to show the actual flow of the WBGT index. The obtained data will be compared to the standard of the WBGT exposure limits from ISO7243 (1982), based on the WBGT-index (wet bulb globe temperature**).** Comparisons were also made using the American Conference of Governmental Industrial Hygienists (ACGIH) (Table 1).

i Workplace Limits and Surveillance

a. Recommended Limits

- Unacclimatized workers: Total heat exposure to workers shall be controlled so that unprotected healthy workers who are not acclimatized to working in hot environments are not exposed to combinations of metabolic and environmental heat greater than the applicable RALs given in Figure 7 (NIOSH, 1986).

- Acclimatized workers: Total heat exposure to workers shall be controlled so that unprotected healthy workers who are acclimatized to working in hot environments are not exposed to combinations of metabolic and environmental heat greater than the application RELs given in Figure 8 (NIOSH, 1986).

- Effect of Clothing: The recommended limits in Figures 7 and 8 are for healthy workers who are physically fit for the level of activity required by their job and who are wearing the customary one layer work clothing ensemble consisting of not more than long-sleeved work shirts and trousers (or equivalent). The RELs and RALs given in Figures 7 and 8 may not provide adequate protection if workers wear clothing with lower air and vapour permeability or insulation values greater than those for the customary one layer work clothing ensemble discussed above (NIOSH, 1986).

- Ceiling Limits: No worker shall be exposed to combinations of metabolic and environmental heat exceeding the applicable Ceiling Limits (C) of Figures 7 and 8 without being provided with and properly using, appropriate and adequate heat-protective clothing and equipment (NIOSH, 1986).

Table 1: Screening Criteria for Heat Stress Exposure (WBGT values in Degree Celsius (^{o}C)) for 8 hour work day five days per week with conventional breaks (Source: OSHA (2008)).

	Acclimatized (^{o}C)				Unacclimatized (^{o}C)			
Work Demands Work : Rest	Light	Moderate	Heavy	Very Heavy	Light	Moderate	Heavy	Very Heavy
100% : 0%	29.5	27.5	26.0	-	27.5	25.0	22.5	-
75% : 25%	30.5	28.5	27.5	-	29.0	26.5	24.5	-
50% : 25%	31.5	29.5	28.5	27.5	30.0	28.0	26.5	25
25% :50%	32.5	31.0	30.0	29.5	31.0	29.0	28.0	26.5

Notes

Rest - sitting (quietly or with moderate arm movements)

Light work - sitting or standing to control machines; performing light hand or arm work (e.g. using a table saw); occasional walking; driving.

Moderate work - walking about with moderate lifting and pushing or pulling; walking at moderate pace; e.g. scrubbing in a standing position

Heavy work - pick and shovel work, digging, carrying, pushing/pulling heavy loads; walking at fast pace; e.g. carpenter sawing by hand

Very Heavy - very intense activity at fast to maximum pace; e.g. shoveling wet sand

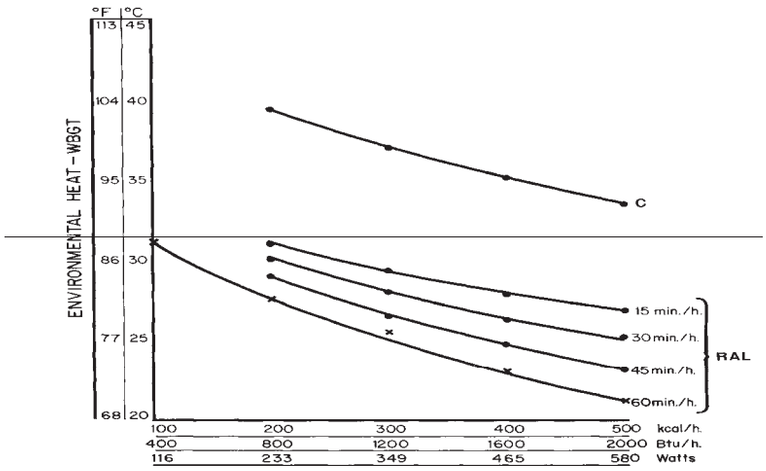

C = Ceiling Limit
RAL = Recommended Alert Limit
For standard worker of 70kg body weight and 1.8m^2 body surface

Figure 7: Recommended Heat-Stress Alert Limits (Heat-unacclimatized workers) (Source: NIOSH (1986)).

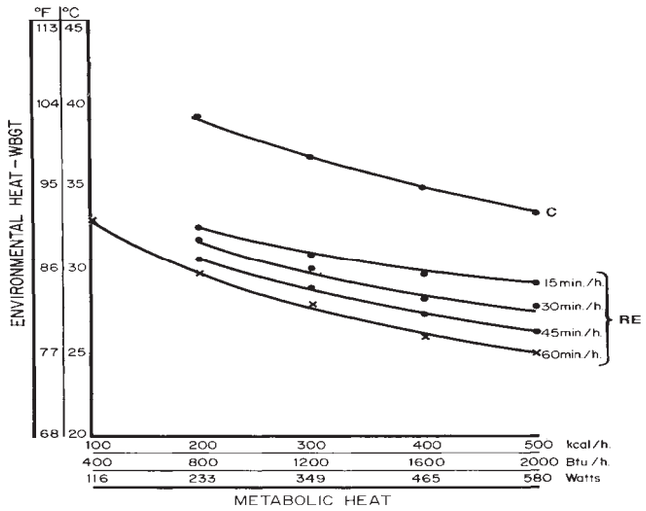

C = Ceiling Limit
REL = Recommended Alert Limit
For standard worker of 70kg body weight and 1.8m^2 body surface

Figure 8: Recommended Heat-Stress Alert Limits (Heat-acclimatized workers) (NIOSH, 1986).

5. RESULTS AND DISSCUSSION

5.1 Main Battle Tank PT-91

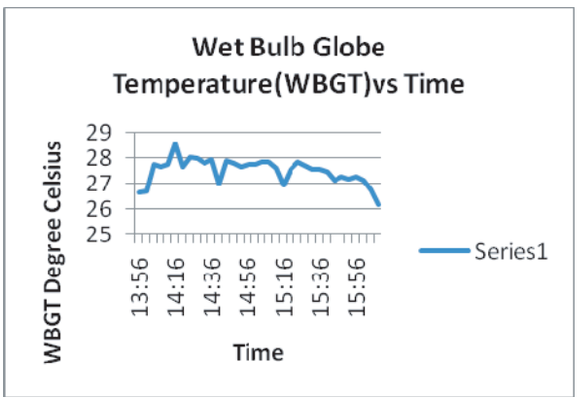

Figure 9 : PT-91 WBGT graph.

The graph in Figure 9 (STRIDE, 2007a) shows that the interior MBT PT-91 vehicle temperature was in an unstable condition. Some points decreased in temperature values, and increased again in a few seconds. The highest point was at 28.56^{o}C at 2 pm and, for most of the time, the temperature was within the range of 27.5 to 28^{o}C. After a few minutes, the temperature dropped to under 27.5^{o}C and remained

until measurement was completed. The polarization of the graph tends to be towards the lower temperature after the peak value. Based on Table 1, the driver is still allowed to drive for about 8 hours without rest.

5.2 Track Logistic carrier (TLC) (Without air conditioning system)

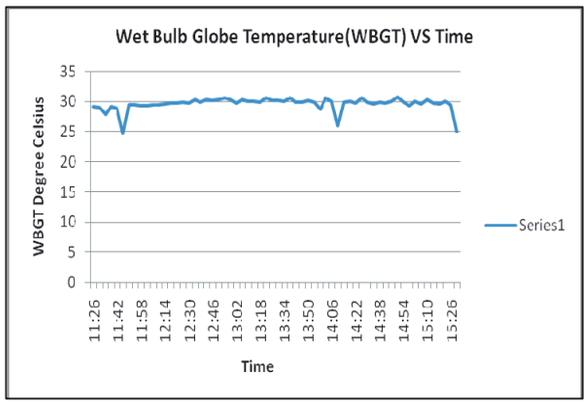

Figure 10: TLC WBGT graph.

The graph in Figure 10 (STRIDE, 2005) shows that the interior TLC vehicle temperature was almost in stable condition at 30°C but the temperature was very high and showed no tendency to decrease. After a few minutes of measurement, the temperature decreased to 24.71°C, and increased again in a few minutes. The temperature was in a stable condition for about 2 hours within the range of 29.0 to 30.5°C. The temperature surged again at 26.04°C and increased again in a few minutes to the mentioned stable range. Based on Table 1, the driver is required to have 25% rest and 75% work.

5.3 Vamtac 4x4 (without Air Conditioning System)

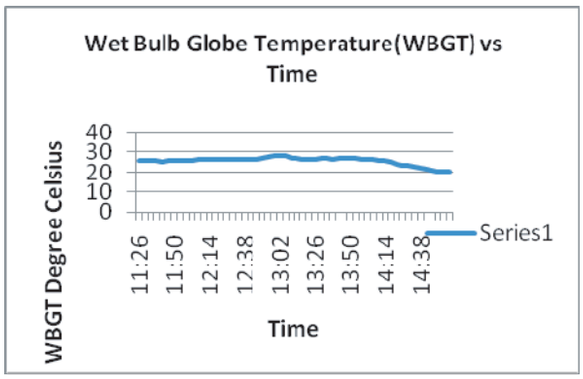

Figure 11: Vamtac WBGT graph.

The graph in Figure 11 (STRIDE, 2007d) shows that for most of the time, the temperature was between 25°C and 30°C for almost 3 hours. The highest point was 28.60°C at 1 pm. The polarization of the graph seems to decrease slowly until the lowest temperature recorded at 20.15°C. Based on Table 1, the driver is still allowed to drive for about 8 hours without rest.

5.4 Tatra 7 Ton

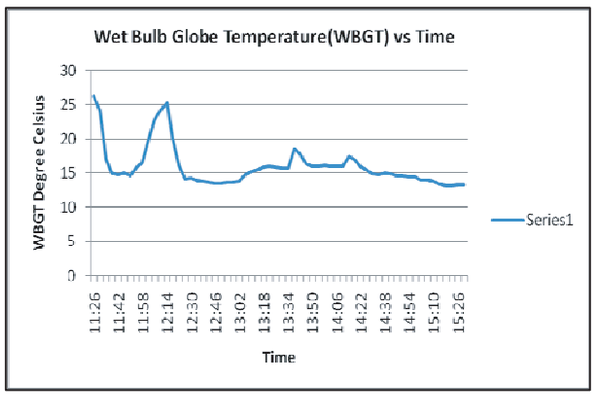

Figure 12: Tatra 7 Ton WBGT graph.

The graph in Figure 12 (STRIDE, 2007b) shows that the temperature had cooled down enough to cover up the entire space inside the vehicle. The highest temperature was at 25^{o}C before it went down to 15^{o}C. For most of the time, the temperature remained stable between 14^{o}C to 17^{o}C. The air conditioning system seemed to be working very well, and therefore, the system was capable of maintaining its temperature. Based on Table 1, the driver is still allowed to drive for about 8 hours without rest.

5.5 Tatra 10 Ton

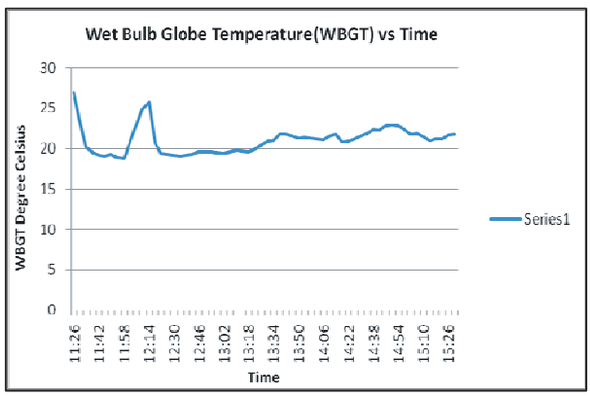

Figure 13: Tatra 10 Ton WBGT graph.

The graph in Figure 13(STRIDE, 2007c) has a similar pattern with the Tatra 7 Ton. However, the system can only maintan its temperature between 19^{o}C to 23^{o}C, as compared to the Tatra 7 Ton which was between 14^{o}C to 17^{o}C. The graph polarization increased from 12 noon to 2 pm. Since there was no dramatic increase in temperature, we may consider that the temperature inside this vehicle to be good. From Table 1, the driver is still allowed to drive for about 8 hours without rest.

6. CONCLUSION

The PT-91 has to be equipped with a good air-conditioning system to ensure the internal temperature is within the comfort zone of 20^{o}C to 25^{o}C. The interior design of Main Battle Tank PT91 has been designed for ammunition and for other tactical purposes. The existence of many partitions may block the flow of the air conditioning of which the blower is located at the front of a dashboard. The use of materials such as ballistic welded steel RHA and composite armour will absorb heat and cause the hall surfaces to become hot. This will generate heat to the internal space of the MBT. Thermal emissions from running gears will also generate heat. All these factors contribute to high temperatures.

The internal heat stress of the Track Load Carrier (TLC) was measured without an air conditioning system. A transducer was placed at the driver compartment. With all doors opened, the vehicle was able to maintain its temperature at about 30^{o}C. This shows that the ventilation is adequate to maintain the temperature. The value of WBGT was quite high, and hence, an air conditioning system is compulsory for this type of vehicle in Malaysian climate.

The internal heat stress of the Vamtac 4x4 was measured without an air conditioning system. A temperature was obtained below 30^{o}C but higher than 25^{o}C. Even though the WBGT was lower than 30^{o}C, an air conditioning system is compulsory to keep a temperature within a comfort zone of 20^{o}C to 25^{o}C.

The WBGT graphs for Tatra 7 Ton and 10 Ton were almost similar in pattern. The air conditioning systems in both vehicles performed very well. This is because the design of both vehicles is similar to the design of a commercial truck. A smaller compartment with a good air conditioning system contributes to a lower WBGT.

In conclusion, total heat stress can be reduced only by modifying one or more of the following factors; metabolic heat production, heat exchange by convection, heat exchange by radiation, and heat exchange by evaporation. Environmental heat load can be modified by engineering controls such as ventilation, air conditioning, screening, insulation, and modification of process or operation.

In Malaysia, the temperature can reach up to 40^{o}C on sunny days. Hence, it is compulsory to provide each military vehicle with an air conditioning system. Failure to do so will cause serious health problems to MAF personnel. Heat disorders such as heat stroke, heat exhaustion, heat cramps, fainting and heat rash may happen to our army personnel if the necessary precautions are neglected. We do not want our military to fail to fight an enemy just because of loss of energy while fighting the heat threat.

ACKNOWLEDGEMENT

The Authors would like to convey special gratitude to Dr. Zalini binti Yunus, Head of the Human Factor Branch, for her valuable advice in writing this paper.

REFERENCES

CCOHS (1997). Hot Measurement-Control Measures. Available online at: http://www.ccohs.ca/oshanswers/phys_agents/heat_control.html. (Last access date: 18th July 2008).

ISO 7243 (1982). Hot Environments- Estimation of the Heat Stress on Working Man, Based on the Wet Bulb Globe Temperature (WBGT) Index

NIOSH (1986). Occupational Exposure to Hot Environments.

Null, J. (2003). Hyperthermia Fatalities. Available online at: http://ggweather.com/heat/hyperthermia2003.htm (Last access date: 15th August 2008)

OSHA (2008). Occupational Safety and Health Administration. Available online at: http://www.osha.gov (Last access date: 16th July 2008).

STRIDE (2007a). Laporan Ujinilai Kenderaan PT91M.

STRIDE (2007b). Laporan Ujinilai Kenderaan Tatra 7 Ton.

STRIDE (2007c). Laporan Ujinilai Kenderaan Tatra 10 Ton.

STRIDE (2007d). Laporan Ujinilai Kenderaan Vamtac 4x4.

STRIDE (2005). Laporan Ujinilai Tanpa Kos dan Obligasi Kenderaan Doosan Tracked Load Carrier.

FLOODING SIMULATIONS FOR NATURAL DISASTER MANAGEMENT AND RELIEF

Dinesh Sathyamoorthy

Instrumentation and Electronic Technology Division
STRIDE, Ministry of Defence, Malaysia
Tel: 603-87324431
Fax: 603-87348695
E-mail: dinsat60@hotmail.com

Abstract

Natural disaster relief efforts have never really been considered as a primary mission for any military. There are no clear guidelines as to the specific role of the Malaysian Armed Forces (MAF) in natural disaster relief. However, in practice, the MAF plays a preeminent role in disaster relief operations. The development of effective natural disaster simulation and modeling tools is important for natural disaster relief as it can help decision makers to understand the systemic effects within a single incident and more complex scenarios about interdependencies between critical incidents happening simultaneously at different locations, provides a platform for local and overall predictions of natural disasters from tracking convenient parameters, and allows for the estimation of damage and losses on both scenario and probabilistic bases. The Science and Technology Research Institute for Defence (STRIDE) is currently working on developing natural disaster simulation and modeling tools for the purposes of natural disaster management and relief. The initial stage of this study concentrates on the characterisation of various geometrical properties of simulated droughts and floods of water bodies. This paper demonstrates the results obtained from the characterisation of influence zones of simulated droughts and floods of water bodies.

Keywords: *Natural disaster management and relief; Natural disaster simulation and modeling tools; Water bodies; Simulated droughts and floods; Influence zones.*

1. INTRODUCTION

In recent years, natural disasters have been affecting increasing numbers of people throughout the world. The Bam earthquake in December 2003 in the Islamic Republic of Iran, the heat-wave that affected Western Europe in 2003, the devastation caused by Hurricanes Ivan and Jeanne in Grenada and other Caribbean countries in September 2004, the Indian Ocean earthquake and tsunami in December 2004, Hurricane Katrina in USA in August 2005, and the Kashmir earthquake in October 2005 accounted for more than 350,000 deaths and USD 194 billion of economic damage between them (UN/ISDR, 2007; EM-DAT, 2008). More recently, cyclone Nargis, which occurred in Myanmar on 2nd May 2008, has caused catastrophic destruction and at least 130,000 fatalities with thousands more people still missing. The Burmese government's official death toll is grossly underreported as they have simply stopped counting the dead to minimize political fallout. It is feared, and is quite possible, those due to lack of relief efforts, a total of 1.5 million people already have or will die from this catastrophe (BBC, 2008a). The Sichuan earthquake, which occurred in the Sichuan province, China on 12 May 2008, has caused a death toll of 69,197 (as of July 6, 2008 12:00 CST). The earthquake left about 4.8 million people homeless, though the number could be as high as 11 million (BBC, 2008b). Given the increase in frequency and seriousness of natural disasters around the globe, efforts to establish better preparedness for and prevention of disasters have been a priority concern of donor agencies, implementing agencies and affected countries.

Tables 1 to 4, obtained from Emergency Disasters Database (EM-DAT, 2008), provide a general summary of natural disasters that have occurred in Malaysia from 1965 to 2007. It is observed that the most frequently occurring natural disaster in Malaysia is floods. Other natural disasters that have affected Malaysia include landslides, windstorms, wild fires, epidemics and tidal-waves.

Table 1: Summarized table of natural disasters in Malaysia from 1965 to 2007. (Source: EM-DAT (2008))

	# of Events	Killed	Injured	Homeless	Affected	Total Affected	Damage US$ (000's)
Drought	1	0	0	0	5,000	5,000	0
avg per event		0	0	0	5,000	5,000	0
Epidemic	11	462	0	0	10,363	10,363	0
avg per event		42	0	0	942	942	0
Flood	30	281	0	35,000	1,111,650	1,146,650	136,700
avg per event		9	0	1,167	37,055	38,222	4,557
Slides	4	152	35	250	0	285	0
avg per event		38	9	63	0	71	0
Wave / Surge	1	80	767	4,296	0	5,063	500,000
avg per event		80	767	4,296	0	5,063	500,000
Wild Fires	2	0	0	3,000	0	3,000	0
avg per event		0	0	1,500	0	1,500	0
Wind Storm	6	294	26	3,000	52,805	55,831	0
avg per event		49	4	500	8,801	9,305	0

Table 2: Top 10 natural disasters in Malaysia (Numbers killed). (Source: EM-DAT (2008))

Disaster type	Date	No Killed
Wind Storm	26-Dec-1996	270
Epidemic	1991	263
Epidemic	Sep-1998	105
Wave / Surge	26-Dec-2004	80
Slides	11-Dec-1993	72
Flood	26-Dec-1970	61
Epidemic	Jul-2007	56
Flood	Jan-1967	50
Slides	30-Aug-1996	50
Flood	22-Dec-1993	30

Table 3: Top 10 natural disasters in Malaysia (Numbers affected). (Source: EM-DAT (2008))

Disaster type	Date	No Affected
Flood	3-Dec-1965	300,000
Flood	26-Dec-1970	243,000
Flood	Jan-1967	140,000
Flood	19-Dec-2006	100,000
Flood	12-Jan-2007	100,000
Flood	12-Nov-1988	60,000
Wind Storm	6-Nov-2004	40,000
Flood	23-Nov-2005	30,000
Flood	28-Nov-1986	25,000
Flood	22-Dec-1993	25,000

Table 4: Top 10 natural disasters in Malaysia (Economic damage). (Source: EM-DAT (2008))

Disaster type	Date	Damage US* (000's)
Wave / Surge	26-Dec-2004	500,000
Flood	26-Dec-1970	37,000
Flood	12-Jan-2007	28,600
Flood	Jan-1967	25,600
Flood	19-Dec-2006	22,000
Flood	28-Nov-1986	11,500
Flood	10-Dec-2004	10,000
Flood	3-Dec-1965	1,000
Flood	21-Nov-2000	1,000
Wind Storm	7-Jan-1968	0

It is important for any country to establish effective natural disaster management policies in order to rationalise decision making for disaster preparedness, provide an objective base for vulnerability assessment and priority setting, and allow for a more effective co-ordination and a more rational approach to natural disaster relief (Allison, 1993; Kreimer, 2000; UN/ISDR, 2007). The emphasis of modern day natural disaster management is on preparedness and a "pro-active" response to replace ad hoc reactive approach of the past (Bildan, 2003; UN/ISDR, 2007).

In Malaysia, the National Disaster Management and Relief Committee, which is chaired by the Deputy Prime Minister, Y.A.B. Dato' Seri Najib Tun Razak, acts as the national mechanism for coordination of disaster management activities (Figure 1). This committee is multidisciplinary in nature and involves representatives from different sectors involved in disaster reduction and emergency management including the Malaysian Armed Forces, the Royal Malaysian Police, the Fire and Rescue Services Department, and volunteer organisations. Every state and district in Malaysia is required to have a natural disaster committee, which is headed by the respective chief ministers and district officers. A detailed explanation on responsibilities of the committee, in policy development, and disaster and post-disaster coordination, is provided in Yassin (2001).

(a) **(b)**

Figure 1: The National Disaster Management and Relief Committee, chaired by the Deputy Prime Minister, Y.A.B. Dato' Seri Najib Tun Razak.

2. ROLE OF THE MALAYSIAN ARMED FORCES IN NATURAL DISASTER RELIEF

Natural disaster relief efforts have never really been considered as a primary mission for any military (Schrader, 1993; Bay, 2005; Witt, 2006). There are no clear guidelines as to the specific role of the Malaysian Armed Forces (MAF) in natural disaster relief. However, in practice, the MAF plays a preeminent role in disaster relief operations (Tan & Boutin, 2001; Acharya *et al*., 2006; Azvee, 2007; Singaravelu, 2007) (Figure 2). In general, the MAF's missions during disasters involve 3 kinds of support:

i. Special functional skills and equipment that support specific response operations
   a. Transportation (trucks, helicopters, boats and other off-road vehicles)
   b. Military construction equipment (e.g. Constructing temporary housing and restoring a minimal essential infrastructure (water, sanitation and communications))
   c. Search and rescue operations (e.g. Victims in collapsed buildings)
   d. Establishing mobile hospitals
   e. Surveillance and reconnaissance (Collecting information and information from isolated areas)
   f. Situation and damage assessment

ii. Communications (that be used to augment the limited survivable local communications)
   a. Equipment and trained personnel

iii. Organized forces (e.g. Assisting medical teams)
   a. Equipment and disciplined personnel

All these are primary military tasks, and hence, the MAF is able to provide this support with little level of preparedness, and on an immediate basis. The MAF's pre-disaster activities include participating in planning, conducting training and earmarking specific types of equipment for support operations, which is a commitment that will ensure that individuals and units receive adequate training, resources and recognition for their disaster response role.

Figure 2: The MAF plays a preeminent role in disaster relief operations

3. NATURAL DISASTER SIMULATION AND MODELING

Recent natural disasters have highlighted the limitations of current response systems, including the lack of interoperability (Bohara *et al.*, 2003; Jain & McLean, 2005, 2006). Effective emergency response presents a number of challenges to the responsible agencies, including the MAF. The development of effective natural disaster simulation and modeling tools is important for natural disaster relief as it can help decision makers to understand the systemic effects within a single incident and more complex scenarios

about interdependencies between critical incidents happening simultaneously at different locations, provides a platform for local and overall predictions of natural disasters from tracking convenient parameters, and allows for the estimation of damage and loses on both scenario and probabilistic bases (Zeng & Kurtz, 1997; Greasley, 2004; Serra, 2007).These simulation and modeling techniques can help address many of the challenges brought forth by the need for emergency response preparedness. Recent surveys (Zeng & Kurtz, 1997; Jain & McLean, 2005, 2006; Serra, 2007) indicate that a number of modeling and simulation applications for analysing various disaster events exist. The integration of simulation models developed independently presents a daunting challenge in itself. Interoperability standards need to be defined that will allow the conforming models and data sources to be integrated. Standards are required for data, architecture and interactions between the models. The interoperability of individual efforts will allow a tremendous synergistic increase in the effectiveness of the emergency response modeling and simulation capability.

The Science and Technology Research Institute for Defence (STRIDE) is currently working on developing natural disaster simulation and modeling tools for the purposes of natural disaster management and relief. The initial stage of this study concentrates on the characterisation of various geometrical properties of simulated droughts and floods of water bodies.

During flooding processes, randomly situated water bodies of varying sizes and shapes tend to self organise. At high degrees of flooding intensity, water bodies contact together to form influence zones, which indicate the self organised criticality of the flooding of water bodies (Sagar, 2001, 2005, 2007). The characterisation of water bodies and their influence zones provides useful insight into the geomorphic properties of a terrain. Sagar (2007) performed the characterisation of water bodies and their influence zones, and found that they follow the universal scaling laws found in other geophysical and biological contexts. However, this study was made with the assumption that water bodies are static objects; they remain constant over time. Water bodies are actually dynamic objects; they go through significant spatio-temporal changes due to droughting and flooding. Dinesh (2007, 2008) proposed a methodology to characterise the influence zones of simulated droughts and floods of water bodies. This methodology is demonstrated in this paper.

4. CHARACTERISATION OF INFLUENCE ZONES OF SIMULATED DROUGHTS AND FLOODS OF WATER BODIES

4.1 The Data Set

Gothavary River, which lies in central India, originates near Triambak in the Nasik district of Maharashtra, and flows through the states of Madhya Pradesh, Karnataka, Orissa and Andhra Pradesh. Although its point of origin is just 80 km away from the Arabian Sea, it journeys 1,465 km to empty into the Bay of Bengal. Some of its tributaries include Indravati, Manjira, Bindusara and Sarbari. Some important urban centers on its banks include Nasik, Aurangabad, Nagpur, Nizamabad, Rajahmundry, and Balaghat. The Gothavary River is often referred to as the Vriddh (Old) Ganga or the Dakshin (South) Ganga. The Gothavary River catchment has an area of 312, 870 km^2 and receives more than 85% of its annual rainfall during the monsoon season (June-September). Hence, the water resource in this river is largely due to monsoon rainfall and largely affected by monsoon extremities, resulting in floods during some years and droughts during others.

Figure 3(a) shows a number of water bodies of varying shape and sizes situated in a portion of the floodplain region of Gothavary River. The water bodies were traced from Indian Remote Sensing Satellites (IRS) 1D remotely sensed data. The IRS-1D was launched on 28 September 1997 by the Indian

Space Research Organization (ISRO) operated Polar Satellite Launch Vehicle (PSLV). The data was captured using the multispectral Linear Imaging Self-Scanning Sensor 3 (LISS-3) with spatial resolution 23.7 m and band range of 520-590 nm. Due to the impracticalities of dealing with incomplete water bodies, only the complete water bodies are considered (Figure 3(b)). A total of 67 distinct individual water bodies (Figure 3(c)) are identified using the connected component labeling (Pitas, 1993).

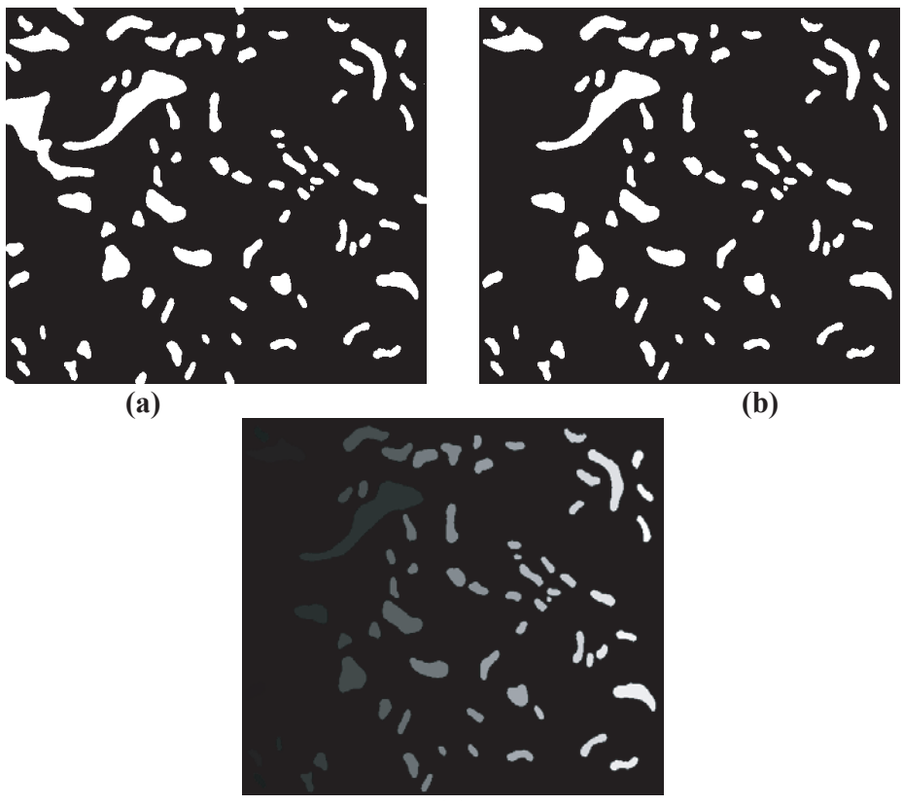

Figure 3: Water bodies of varying shape and sizes situated in a portion of the flood plain region of Gothavary River. (a) The original water bodies traced from IRS 1D remotely sensed data. (b) The water bodies after removal of incomplete water bodies. (c) Identification of the individual water bodies using connected component labeling. The water body count number is determined by the grey level; the brighter the grey level, the larger the water body count number.

4.2 Generation of Simulated Droughts and Floods using Mathematical Morphology

Mathematical morphology is a branch of image processing that deals with the extraction of image components that are useful for representational and descriptional purposes. Mathematical morphology has a well developed mathematical structure that is based on set theoretic concepts. The effects of the basic morphological operations can be given simple and intuitive interpretations using geometric terms of shape, size and location. The fundamental morphological operators are discussed in Matheron (1975), Serra (1982) and Soille (2003). Morphological operators generally require two inputs; the input image A, which can be in binary or grayscale form, and the kernel B, which is used to determine the precise effect of the operator.

Dilation sets the pixel values within the kernel to the maximum value of the pixel neighborhood. Binary dilation gradually enlarges the boundaries of regions of foreground pixels, resulting in areas of foreground pixels growing in size, and holes within those regions becoming smaller (Duchane & Lewis, 1996). The dilation operation is expressed as:

$$A \oplus B = \{a+b: a \epsilon A, b \epsilon B\} \quad (1)$$

Erosion sets the pixels values within the kernel to the minimum value of the kernel. Binary erosion gradually removes the boundaries of regions of foreground pixels, resulting in areas of foreground pixels shrinking in size, and holes within those areas becoming larger (Duchane & Lewis, 1996). Erosion is the dual operator of dilation:

$$A \ominus B = (A^c \oplus B)^c \quad (2)$$

where A^c denotes the complement of A, and B is symmetric with respect to reflection about the origin.

Drought and flood simulation is implemented by performing erosion and dilation, respectively, on water bodies using square kernels of increasing size. Erosion reduces the area of water bodies, mimicking droughting, while dilation increases the area of water bodies, mimicking flooding. The level of droughting/flooding is indicated by the kernel size.

Simulated droughts (Figure 4) and floods (Figure 5) of the water bodies for levels of 1 to 15 are computed. The areas of the generated simulated droughts and floods are shown in Table 5.

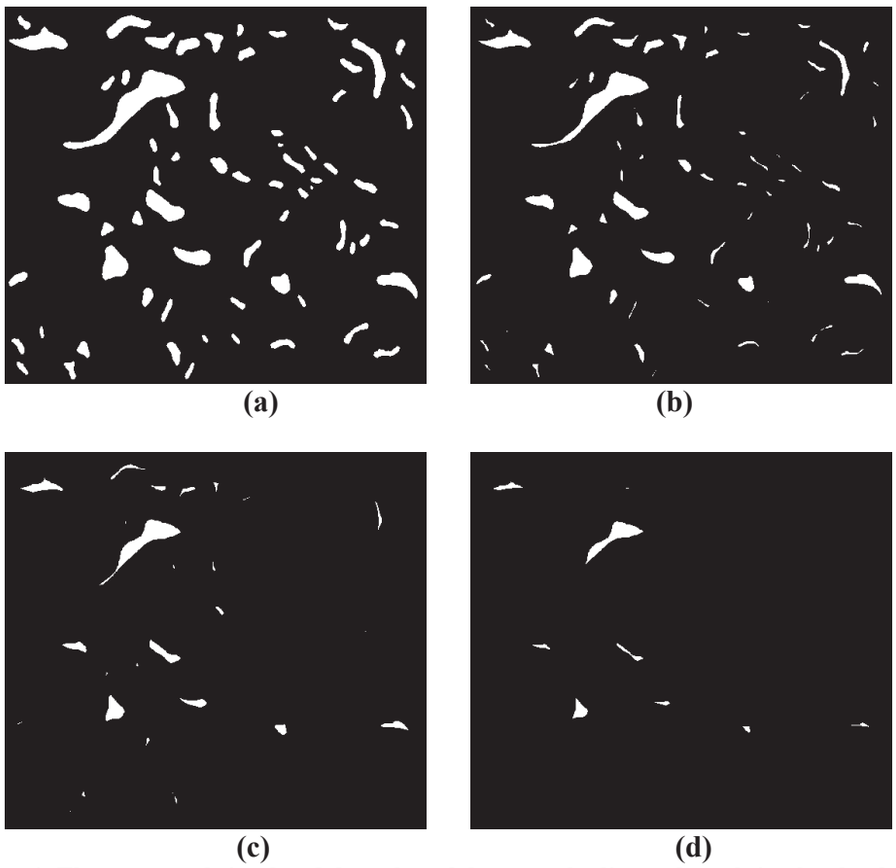

Figure 4: The generated simulated droughts of the water bodies at droughting levels of: (a) 3 (b) 7 (c) 11 (d) 15.

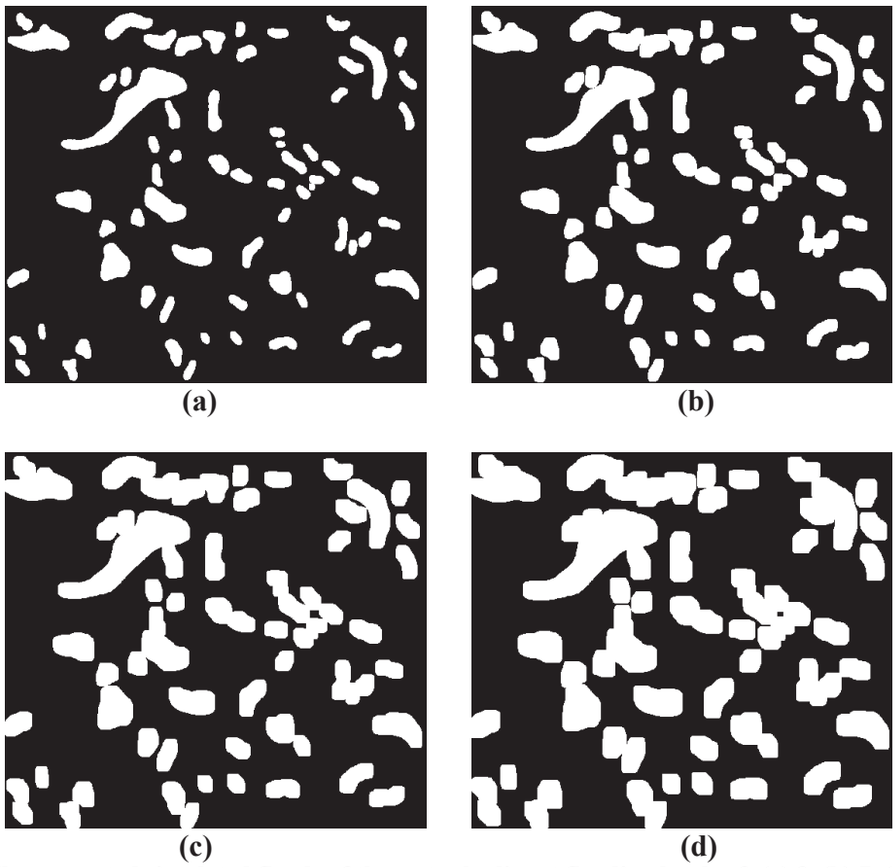

Figure 5: The generated simulated floods of the water bodies at flooding levels of: (a) 3 (b) 7 (c) 11 (d) 15.

Table 5: Areas of the generated simulated droughts and floods of water bodies.

Level	Area (pixels)	
	Drought	Flood
1	137837	137837
2	123336	152789
3	109565	167979
4	96328	183647
5	83764	199532
6	71844	215862
7	60839	232283
8	51141	249127
9	42863	265919
10	35980	283048
11	30230	300047
12	25380	317358
13	21220	334503
14	17737	351937
15	14794	369093

4.3 Generation of Influence Zones of Simulated Droughts and Floods of Water Bodies

If P_1, P_2… P_n are disjoint sets, then the influence zone of P_i is the locus of those points which are closer to P_i than to any other set. Connected component labeling is implemented on the generated simulated droughts and floods in order to identify the individual water bodies. The influence zones of the generated simulated droughts (Figure 6) and floods (Figure 7) of the water bodies are computed applying the immersion simulation algorithm proposed in Vincent & Soille (1991) on the grayscale images generated using connected component labeling. This algorithm is based on a progressive flooding of an image, is applicable to *n*-dimensional images. The pixels are first sorted in increasing order of their grey levels. The successive grey levels are processed in order to simulate the flooding propagation. A distributive sorting technique combined with breadth-first scannings of each grey level allow for an extremely fast computation of influence zones.

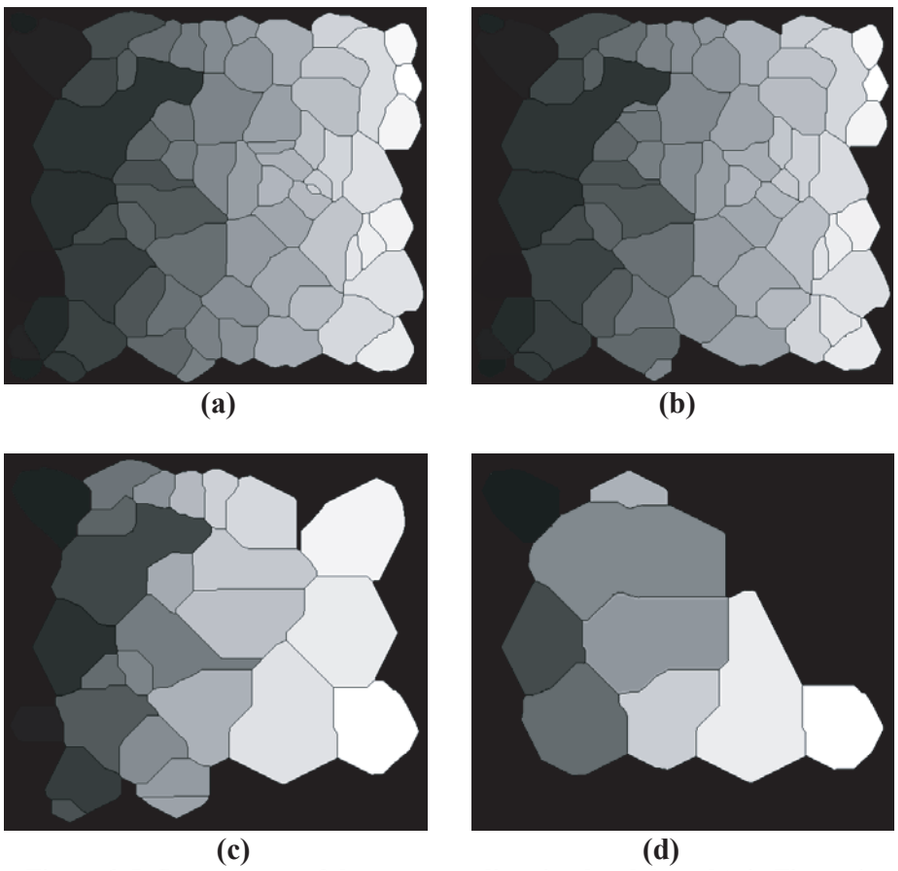

Figure 6: Influence zones of the corresponding simulated droughts in Figure 4.

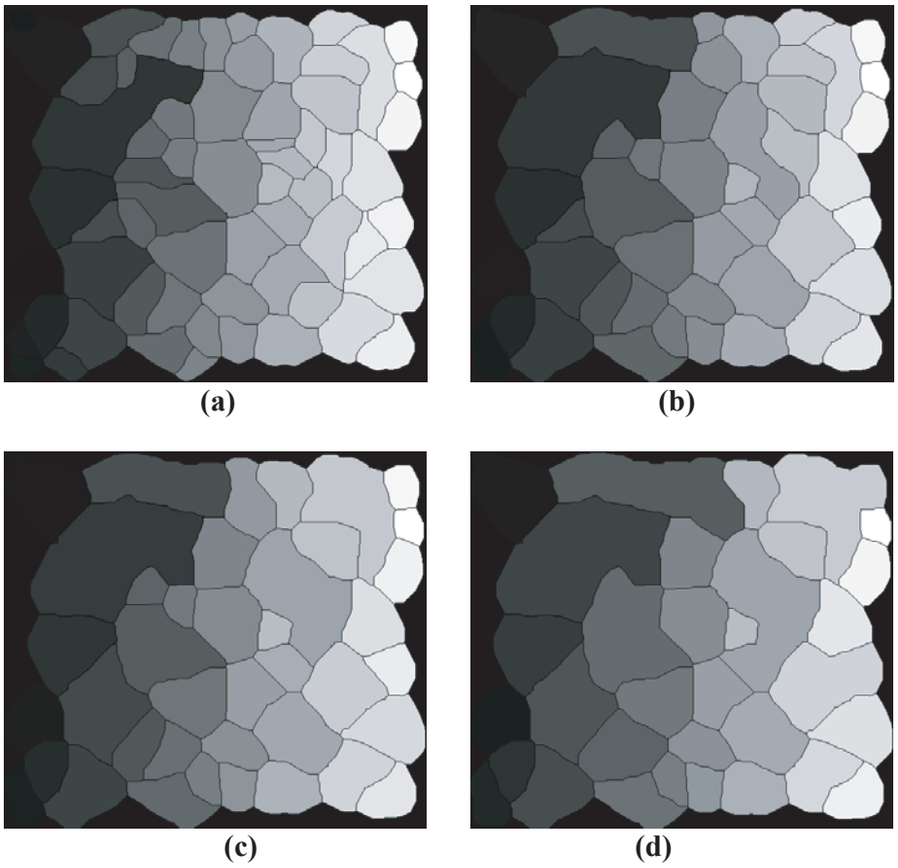

Figure 7: Influence zones of the corresponding simulated floods in Figure 5.

4.4 Results and Discussion

The average areas of the influence zones of the simulated droughts and floods are computed (Table 5). It is observed that as the droughting level increases from 1 to 5, the average area of the influence zones reduces. This occurs as when the level of droughting is increased; the areas of the water bodies reduce, resulting in a decrease in the average area of the generated influence zones.

As the droughting increases from 5 to 15, the average area of the influence zones of water bodies increases. This occurs as when the level of droughting is increased, a number of small water bodies vanish, resulting in a decrease in the number of influence zones, and hence, an increase in the average area of the influence zones.

It is also observed that as the level of flooding increases, the average area of influence zones of water bodies increases. This occurs as when the level of flooding is increased, the level of merge between adjacent water bodies increases, resulting in a decrease in the number of influence zones, and hence, an increase in the average area of the influence zones.

Table 5: Average areas of influence zones of the simulated droughts and floods of water bodies.

Level	Average area of influence zones (pixels)	
	Drought	Flood
1	3394.62	3394.62
2	3327.96	3517.67
3	3312.55	3590.27
4	3296.93	3992.42
5	3280.81	4234.78
6	3311.53	4506.88
7	3324.31	5135.51
8	3261.03	5400.16
9	3800.54	5551.21
10	5670.41	5710.83
11	6807.22	5875.85
12	7451.82	6048.87
13	9154.00	6401.19
14	11689.67	6997.44
15	13976.33	7235.39

A log-log plot of the average area of the influence zones of the simulated floods *S* against the level of flooding *r* is drawn (Figures 8). Two log-log plots of the average area of the influence zones of the simulated droughts *S* against the level of droughting *r* are drawn, one for droughting levels of 1 to 5 (Figure 9a), and one for droughting levels of 5 to 15 (Figure 9b). Power law relationships are observed in all three plots. These power laws take the following form:

$$S = c * r^{D} \quad (3)$$

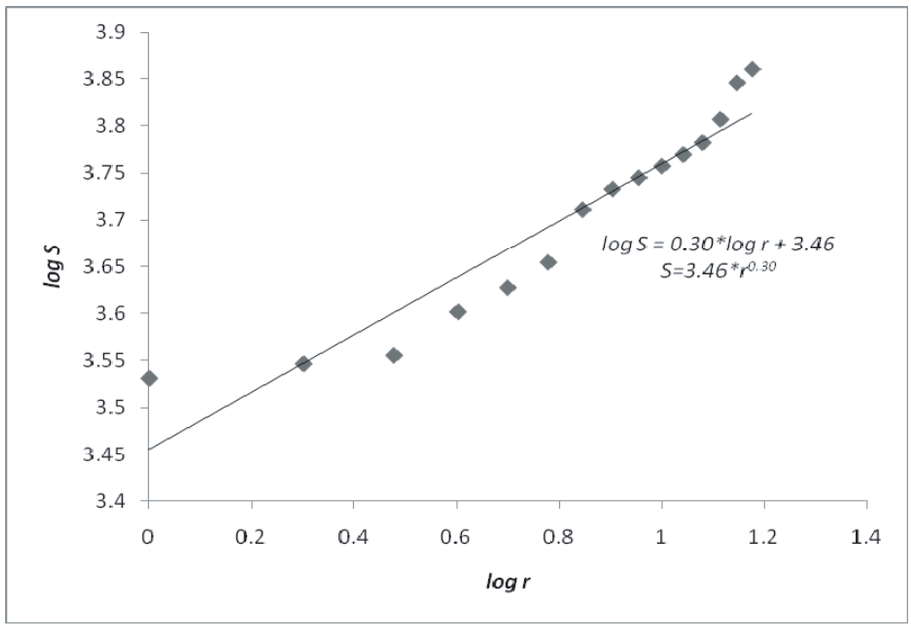

Figure 8: Log-log plot of the average area of the influence zones of the simulated floods against the flooding level.

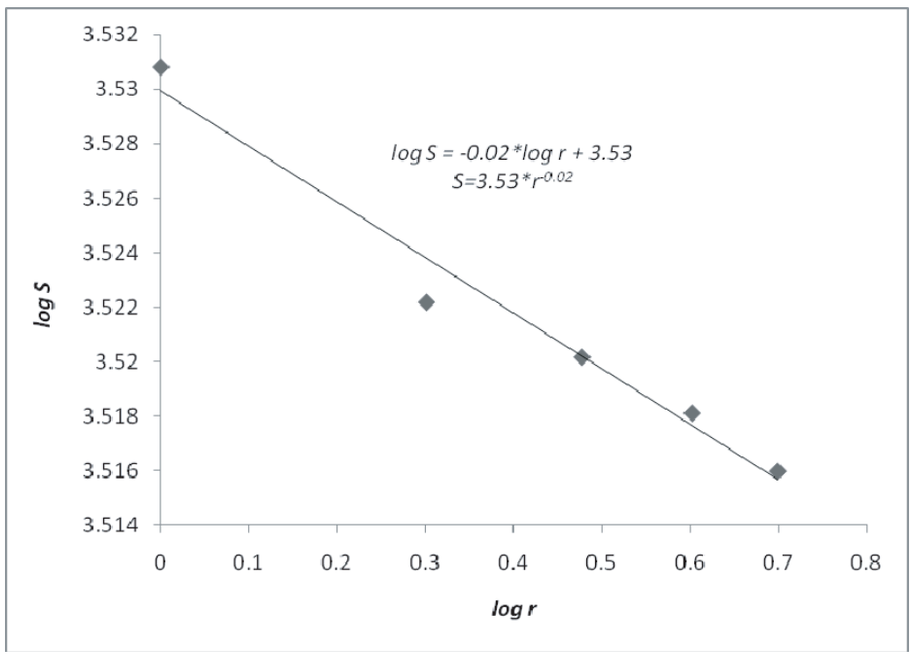

(a)

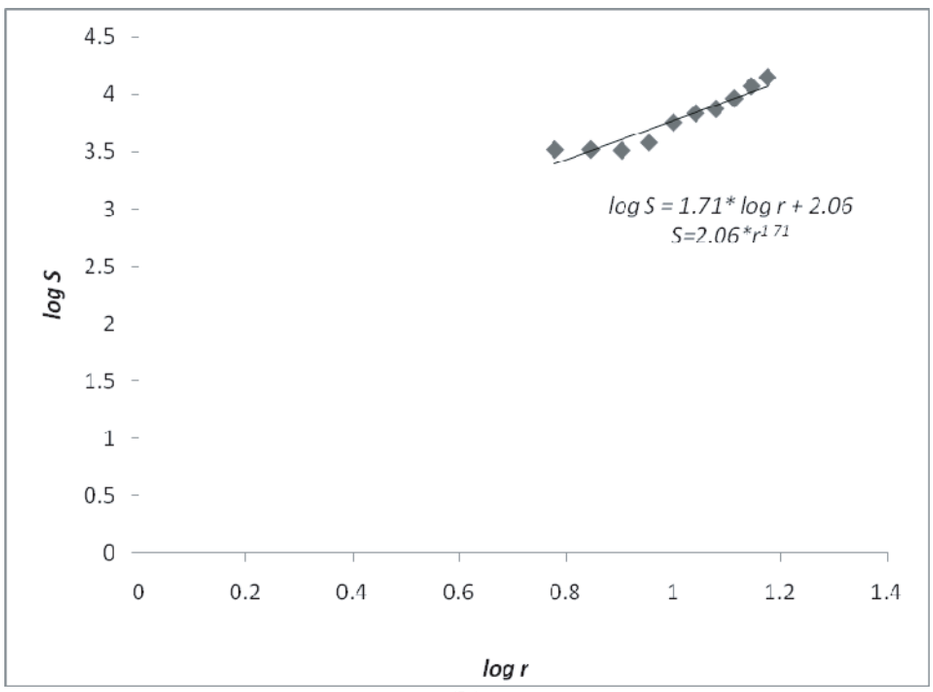

(b)

Figure 9: Log-log plots of the average area of the influence zones of the simulated droughts against the droughting level. (a) For droughting levels of 1 to 5. (b) For droughting levels of 5 to 15.

These power law relationships arise as a consequence of the fractal properties of the influence zones of simulated droughts and floods of water bodies. The term 'fractal' implies that an object or pattern has self-similar or self-affine properties. Self-similar means that parts of an object are identical to the whole, and self-affine means that parts of an object resemble systematically squashed or stretched versions of the wholes. Ideal fractals display similarity across an infinite range of scales, which is rarely seen in nature. Consequently, the ranges of fractality can be used to decipher characteristic scales and thresholds at which physical processes operate. Fractal geometry was introduced and popularised by Mandelbrot (1967, 1977, 1988) to describe highly complex forms that are characteristic of natural phenomena such as coastlines and landscapes. In Equation 3, c is a constant of proportionality, while D is the fractal dimension of the average area of the influence zones of simulated droughts/floods of water bodies, which indicates the rate of change of average areas of the influence zones over varying levels of droughting/flooding. D has a positive value for increasing average areas of influence zones, and a negative value for decreasing average areas of influence zones.

5. SCOPE FOR FUTURE WORK

In general, floodplain regions have a maximum gradient of less than 2°. In this paper, droughting and flooding simulations are performed on the assumption that floodplain regions approximate isotropic surfaces. However, this assumption does not hold for other areas with gradients higher than 2°. In these cases, droughting and flooding simulation will need to take into consideration the gradient computed from the corresponding elevation maps. Furthermore, while the study of the Gothavary River floodplain does provide interesting results in regards to a region that undergoes significant spatio-temporal changes due to droughts and floods, the conclusions drawn from the study of this region does not necessarily apply to all regions. At present, work is being done to study the influence zones of simulated droughts and floods of water bodies of regions of varying geomorphological topographies in order to study the generality of the findings of this paper. The findings obtained need to be validated via observations of actual floods and droughts of water bodies through a time series of remotely sensed imagery. In addition to this, the effect of variation in spatial extent and resolution also need to be taken into consideration in order to determine that the observed findings are scale-independent.

ACKNOWLEDGEMENTS

This article is a revised version of the manuscript entitled "Flooding simulations for natural disaster relief" which was presented during the Workshop on Natural Disasters and Simulations, which was held in the Earth Observation Centre (EOC), Universiti Kebangsaan Malaysia (UKM), Bangi, Selangor on 17th September 2007. The author is grateful to Prof. Emeritus Jean Serra, Centre de Morphologie Mathématique, France, and Assoc. Prof. Mastura Mahmd, EOC UKM, for their suggestions that have improved the technical content of this article.

REFERENCES

Acharya, A., Emmers, R. & Caballero-Anthony, M. (2006). Studying Non-traditional Security in Asia: Trends and Issues. Institute of Defence and Strategic Studies, Nanyang Technological University, Singapore.

Allinson, R.E. (1993). Global Disasters: Inquiries into Management Ethics. Prentice Hall, New York.

Azvee, Z. (2007). Disaster Medicine-Malaysian Armed Forces Medical Team (MASMEDTIM) Yogjakarta Earthquake May-June 2006. 17th Annual Asia Pacific Military Medicine Conference, 16th –20th April 2007, Manila, Philippines.

Bay, A. (2005). Military and natural disasters. Strategy Page. Available online at: http://www.strategypage.com/on_point/2005928.aspx (Last access date: 21st July 2008).

BBC News (2008a). Burma cyclone: Mapping the aftermath. Available online at: http://news.bbc.co.uk/2/hi/asia-pacific/7408423.stm (Last access date: 21st July 2008).

BBC News (2008b). China earthquake. Available online at: http://news.bbc.co.uk/2/hi/in_depth/asia_pacific/2008/china_quake/default.stm (Last access date: 21st July 2008).

Bildan, L. (2003). Disaster Management in South East Asia: An Overview. Asian Disaster Preparedness Center, Bangkok.

Bohara, A.S., Collins, T.C., Davis, S.C., Goknur, S.C., Kearns, J.C., T.N., Lieu, Nguyen, T.P., Zeng, J.S., Horowitz, B.M., & Patek, S.D. (2003). Integrated peer-to-peer applications for advanced emergency response system-Part 1: Concept of operations. Proceedings of the 2003 Systems and Information Engineering Design Symposium.

Dinesh, S. (2007). Analysis of influence zones of simulated droughts and floods of water bodies. Joint International Symposium & Exhibition on Geoinformation and GPS/GNSS 2007 (ISG & GPS/GNSS 2007), 5th to 7th November 2007, PERSADA Johor International Convention Centre, The Puteri Pacific, Johor Bahru.

Dinesh, S. (2008). Characterization of influence zones of simulated droughts and floods of water bodies in a flood plain. Computers & Geosciences, In press.

Duchene, P. & Lewis, D. (1996). Visilog 5 Documentation. Noesis Vision, Quebec.

EM-DAT (2008). Emergency Disasters Database. Available online at: http://www.em-dat.net (Last access date: 21st July 2008).

Greasley, A. (2004). Simulation Modelling for Business. Ashgate Press, UK.

Jain, S. & McLean, C. (2005). Integrated Modeling and Simulation for Multiple Phases of Emergency Response. Working together: Research & Development Partnerships in Homeland Security, 27th-28th April 2005, Boston, MA.

Jain, S. & McLean, C. (2006). An Integrating Framework for Modeling and Simulation for Incident Management. Journal of Homeland Security and Emergency Management, 3(1), Article 9.

Kreimer, A. (2000). Managing Disaster Risk in Emerging Economies. World Bank, Washington D.C.

Mandelbrot, B.B. (1967). How long is the coast of Britain? Statistical self-similarity and fractional dimension. *Sci*., **156**: 636-638.

Mandelbrot, B.B. (1977). Fractals: Form, Chance and Dimension. Freeman, San Francisco, California.

Mandelbrot, B.B. (1982). The Fractal Geometry of Nature. Freeman, San Francisco, California.

Matheron, G. (1975). Random Sets and Integral Geometry. Wiley, New York.

Pitas, I. (1993). Digital Image Processing Algorithms. Prentice Hall, London.

Sagar, B.S.D. (2001). Generation of self organized critical connectivity network map (SOCCNM) of randomly situated surface water bodies. *Discrete Dynam. Nat. Soc.*, **6:** 225-228.

Sagar, B.S.D. (2005). Discrete simulations of spatio-temporal dynamics of small water bodies under varied streamflow discharges. *Nonlinear Processes in Geophysics*, **12**: 31-40.

Sagar, B.S.D. (2007). Universal scaling laws in surface water bodies and their zones of influence, Water Resources. 43(2), W02416, doi:W06502,10.1029/2006WR005075.

Schrader, J.Y. (1993). The Army's Role in Domestic Disaster Support: An Assessment of Policy Choices. RAND Monograph Report, Arroyo Center, RAND Corporation, Santa Monica, California.

Serra, J. (1982). Image Analysis and Mathematical Morphology. Academic Press, London.

Serra, J. (2007). Modeling of environmental disasters from RS and GIS data. Workshop on National Disasters and Simulation, 17th September 2007, Earth Observation Centre, Universiti Kebangsaan Malaysia, Bangi, Selangor.

Singaravelu, J. (2007). Bridging borders: The tsunami disaster in Aceh, Indonesia. 17th Annual Asia Pacific Military Medicine Conference, 16th –20th April 2007, Manila, Philippines.

Soille, P. (2003). Morphological Image Analysis: Principles and Applications. Springer Verlag, Berlin.

Tan, A.T.H. & Boutin, J.D. (2001). Non-traditional Security Issues in Southeast Asia. Institute of Defence and Strategic Studies, Nanyang Technological University, Singapore.

United Nations/International Strategy for Disaster Reduction (UN/ISDR), 2007. Disaster Risk Reduction: 2007 Global Review. Global Platform for Disaster Risk Reduction, 5th-7th June 2007, Geneva, Switzerland.

Vincent, L. & Soille, P. (1991). Watersheds in digital spaces: An efficient algorithm based on immersion simulations. *IEEE Trans. Patt. Anal. Mach. Intel.*, **13**: 583-598.

Witt, J.L. (2006). Military Role in Natural Disaster Response. Disaster Preparedness, 1(1), 2-5.

Yassin, M.M. (2001). Pengurusan Bantuan Bencana Negara: Satu Kajian Kes ke Atas Bahagian Keselamatan Negara, Jabatan Perdana Menteri. Masters thesis, Faculty of Economics and Managament, Universiti Malaya, Malaysia.

Zeng, L. & Kurtz, S. (1997). Evaluation of natural disaster models. CAS Seminar of Reinsurance, 1st-3rd June 1997, Bermuda.

OVERVIEW OF TECHNIQUES FOR THE DETECTION AND IDENTIFICATION OF MICRO-ORGANISMS

Zalini Yunus

Protection & Biophysical Technology Division,
Science & Technology Research Institute for Defence (STRIDE),
Taman Bukit Mewah Fasa 9, 43000 Kajang, Selangor D.E.
Tel: 03-87324400
Fax: 03-87348695
Email: yzalini@yahoo.co.uk

Abstract

This paper gives an overview on the advantages and disadvantages of some of the techniques used for the detection, separation, enumeration and identification of micro-organisms. These techniques are categorised into two main groups; conventional methods and recent techniques. Conventional techniques are very sensitive, inexpensive and can give both qualitative and quantitative information on the number and the nature of the micro-organisms present in samples. However, these techniques involve time-consuming and laborious preparation procedures. Meanwhile, recent techniques that have been developed can rapidly detect low concentrations of pathogens either in water, food and clinical samples, nevertheless the capital cost involved usually in certain techniques are high and require highly skilled workers to carry out tests.

Keywords: *Micro-organism; Detection; Enumeration; Identification*

1. INTRODUCTION

Conventional methods for detection and identification of micro-organisms, viruses and/or their products involve time-consuming and laborious preparation procedures such as resuscitation, pre-enrichment, selective enrichment and isolation of cells before a subsequent specific detection or identification can be achieved using further procedures such as biochemical screening and serological confirmation (Tietjen & Fung 1995; Hobson *et al*., 1996). Most of these tests require several days to give results because they rely on the ability of micro-organisms to multiply to give visible colonies. Moreover, culture medium preparation, inoculation of plates, colony counting and biochemical characterisation make these methods labour intensive.

There have been many attempts to modify conventional microbiological techniques in order to achieve a more extensive and quicker analysis of samples, and many types of rapid detection, isolation and enumeration techniques are now available commercially. Rapid methods in microbiology have mainly been developed in the areas of immunology and DNA technology, but some useful improvements of conventional techniques have also been made (Manafi, 1996; de Boer & Beumer, 1999). Few of these approaches have the potential to selectively quantify individual fractions within a mixture without supplementary techniques. Methods commonly applied to cell or particle enumeration, such as conductance or impedance analysis, direct epifluorescense techniques (DEPT), ATP or enzyme assays, cannot yet discriminate between different species. Other instruments and techniques that can differentially enumerate mixed suspensions of bacteria are very expensive or laborious e.g. flow cytometry, fluorescent antibody methods, ELISA.

This paper will present a brief description of the advantages and disadvantages of some of the techniques used for the detection, separation, enumeration and identification of micro-organisms. These techniques are categorised into two main groups; (i) conventional methods and (ii) recent techniques.

2. CONVENTIONAL METHODS FOR DETECTION, IDENTIFICATION AND ENUMERATION OF MICRO-ORGANISMS

Conventional microbiological testing methods rely on specific microbiological media to isolate and enumerate viable cells in samples (e.g. food, water or clinical samples). These methods are very sensitive, inexpensive and can give both qualitative and quantitative information on the number and the nature of the micro-organisms present in samples. However they are greatly restricted by long assay time. Moreover, culture medium preparation, inoculation of plates, colony counting and biochemical characterisation make these methods labour intensive. Here some conventional methods are described.

2.1 Microscopic Techniques

Observation under light microscope could give preliminary information regarding bacterial shape and size, or whether they are Gram-positive or Gram-negative. However, if the micro-organism has no distinctive cell morphology, light microscope will be unable to identify the micro-organism present due to the relatively low magnification of the sample. This limitation is the result of light being diffracted by the object under observation Higher resolution microscopic techniques such as the transmission electron microscope (TEM) and scanning electron microscope (SEM) have been used in the counting, detection and identification of micro-organisms (viruses, bacteria and fungi) (Westall *et al*., 2001; Little *et al*., 2001; Pósfaia *et al*., 2003). Scanning electron microscope is more suitable for determining the surface appearance of microbial cells and can be used to analyse associations between cells, growth habits and in the study of biofilms. The TEM, which has greater resolving power, is also applicable for the detection and identification of viruses (Metcalf *et al*., 1995).

Nevertheless the use of electron microscopic techniques as a low cost rapid method for detection or identification is unlikely due to the high cost of instrumentation, the high operator skill required as well as the difficulty in producing quantitative preparations. Furthermore, the electron microscope can only be used for the examination of dead cells and is therefore unsuitable for the investigation of intracellular movement or transport processes.

Using a scanning confocal laser microscopy (SCLM), a three-dimensional picture of a fluorochrome labelled sample can be generated. The SCLM has been used in the detection of micro-organisms in environmental samples, including the analysis of the *in situ* structure of microbial biofilms (Neu & Lawrence, 1997). The major limitation of the SCLM in biology is its relatively slow acquisition speed especially when working with living cells. The ability to image fluorescent samples at video speed or higher, would be highly desirable (Cox, 2002). In addition, the instrumentation cost is high.

2. 2 Culture-Based Methods

Plate count methods are widely used to estimate microbial populations. Serial dilutions of samples are spread onto agar plates, which are then incubated at the appropriate growth temperature. The number of colonies is counted and multiplied by the dilution factor to obtain the viable count of colony forming units (cfu) per ml in the original sample. When counting anaerobic bacteria, it may be necessary to treat diluents to remove dissolved air prior to use.

Certain media perform better then others in the detection of specific micro-organisms (Rayman *et al*., 1998), yet often time-consuming confirmation tests must be used to obtain reliable results (Niskanen &

Aalto, 1978; Noleto & Bergdoll, 1980). In addition, the common errors associated with microbiological plating are deficiencies in medium composition, the erroneous incubation temperatures and mistakes in calculation of results (Peterz & Steneryd, 1993).

2. 3 Colorimetry-Based Techniques

Colorimetric techniques are based on the use of compounds whose colour is changed in the presence of the micro-organisms.

2. 3.1 *Multiple-tube fermentation technique*

The multiple-tube fermentation (MTF) technique has been used widely to enumerate the presence of coliforms in water without the requirement for direct counting (Jones & Knowles, 1991; Rompré *et al.*, 2002). The technique can be performed by a technician with basic microbiological training. Nevertheless, the method can be tedious and labour intensive since many dilutions have to be processed for each sample. This method is extremely time-consuming and necessitates a subculturing stage for confirmation which could take up to a further 48 hours. Furthermore, interference by high numbers of non-coliform bacteria (Evans *et al.*, 1981; Means & Olson, 1981) as well as the inhibitory nature of the media (McFeters *et al.*, 1982) have been identified as factors contributing to underestimates of coliform abundance. The application of this technique to soil samples requires the extraction of the micro-organisms present into water or buffer.

2. 3.2 *Membrane filter technique*

The membrane filter (MF) technique is widely used as a procedure for monitoring drinking water microbial quality. This method consists of filtering a water sample on a sterile filter with 45 μm pore size which retains bacteria. This filter is then incubated on a selective medium. Typical colonies appearing on the filter are then counted (APHA *et al.*, 1998).

The widely used selective media for drinking water analysis are the m-Endo-type media (APHA *et al.*, 1998) and the Tergitol-TTC medium (AFNOR, 1990). Coliform bacteria form a metallic sheen on an Endo-type medium containing lactose or yellow orange colonies on Tergitol-TTC medium. Enumeration of total coliform by MF is not totally specific because typical colonies with a metallic sheen may be produced occasionally by non-coliform bacteria and, conversely, atypical colonies (dark red or nucleated colonies without sheen) may sporadically be coliforms (APHA *et al.*, 1998). The presence of background heterotrophilic bacteria was shown to decrease coliform recovery by MF (Clark, 1980; Burlingame *et al.*, 1984). Excessive crowding of colonies on m-Endo media has been associated with a reduction in coliform colonies producing the metallic sheen (Hsu & Williams, 1982; Burlingame *et al.*, 1984).

This method however is not specific. Therefore a confirmation stage is needed, which could take a further 24 h after the first incubation period (24 to 48 h) on selective media. Furthermore the method is unable to recover stressed or injured coliforms (Rice *et al.*, 1987; Adams *et al.*, 1989).

2. 4 Turbidity

Turbidity is widely used method for the estimation the number of cells in a suspension as an alternative to traditional plate counts (McMeekin *et al.*, 1993). The turbidity is determined by measuring the light loss from the beam by scattering and absorption (Singh *et al.*, 1994). A standard calibration curve of optical density against either the total count or dry weight is used (McMeekin *et al.*, 1993; Begot *et al.*, 1996). This is then used to determine the number of cells in a suspension from measured turbidity of a sample. Transferring the cells from one medium to another or washing the cells can disturb the osmotic potential

across the cell membrane. This may change the cell surface area/volume ration and refractive index, hence the turbidity without altering the cell count or total mass. The calibration curve applies only to micro-organisms grown under a particular set of growth conditions. If any changes occur in the growth conditions, a new curve must be prepared. In addition, cells grown in high carbohydrate or fat media frequently have a high turbidity (Hobson *et al*., 1996).

3. DESCRIPTION OF SOME RECENT METHODS FOR DETECTION, IDENTIFICATION AND ENUMERATION OF MICRO-ORGANISMS

There is a need for more rapid methods to provide information about the presence of certain micro-organisms in samples such as pathogens. These methods need to deal not only with the early detection and enumeration of micro-organisms, but also with the characterisation of isolates, by the use of microbiological, chemical, biochemical, biophysical, molecular biological immunological, and serological methods (Fung, 1995). Considerable efforts are now directed towards the development of methods that can rapidly detect low concentrations of pathogens in water, food and clinical samples. For this purpose, a number of instruments have been developed using various principles of detection, e.g. chromatography, infrared or fluorescence spectroscopy, bioluminescence, flow cytometry, impedimetry and many others (Hobson *et al*., 1996; Basile *et al*., 1998; Perez *et al*., 1998). These procedures rely on the separation or concentration of the target cells or cell fragments to a detectable level by a non-growth step. The end-detection method does not rely upon an incubation period for colony formation. Table 1 lists examples of technologies which have been applied to improve the detection of bacteria (Olsen, 2000).

The most frequently used rapid and automated methods in industry are enzyme linked immunosorbent assays (ELISA), impedance (or conductance) methods, immunomagnetic separation (IMS) and bioluminescence methods. These techniques may be used on their own or in combination. For example, a rapid separation method such as immunomagnetic separation can be used in conjunction with a rapid end detection method such as ELISA. These methods have been developed either to (a) replace the enrichment step (which requires a prolonged growth period) with a concentration step, such as immunomagnetic separation or (b) to replace the end-detection method, which is usually colony development and hence requires a prolonged incubation period, by a technique such as impedance microbiology or bioluminescence.

Table 1. Examples of the new methods for detection of bacterial (adapted from Olsen, 2000).

Principle	Example of Methodology
Improved viable count	Spiral plate count Hydrophobic grid-membrane filter technique
Microscopy techniques	Direct epifluorescence filter technique (DEFT) Fluorescence antibody technique
Cell counting	Flow cytometry
Changes in electrical properties	Impedimetry methods
Estimation of metabolic activity	ATP assays
Antibody/antigen reaction	Latex agglutination Immunomagnetic separation Enzyme linked immunosorbent assays (ELISA)
DNA-detection	Colony hybridisation Single phase hybridisation assays Polymerase chain reaction (PCR) Oligonucleotide arrays (DNA-disc technology)

Advantages or problems encountered with some recent rapid methods for the detection and identification of micro-organisms will be described below.

3.1 Immunological Based Technique

Immunological methods are based on the specific binding of an antibody to an antigen. A variety of antibodies which have been employed in different assay types have been described (Märtlbauer & Becker, 1995). The suitability of these antibodies depends mainly on their specificity.

3.1.1 *Enzyme-linked immunosorbent assays*

The enzyme-linked immunosorbent assay (ELISA) methods are widely used for the detection or quantification of substances in samples based on an immunological reaction (Kemeny, 1991). For many ELISA methods, the typical response is a colour change of the solution in the well, which is measured by a spectrophotometer. Antibodies are developed to bind specific antigens on the surface of the target micro-organisms, and cause the micro-organisms to become clumped together and visible to the naked eye. The ELISA methods can be used quantitatively to detect the presence of bacteria, fungi and viruses (Nybroe *et a*l., 1990; Hubner *et al*., 1992). However it is not a straightforward method to perform and it is sensitive to non-specific reactions (Notermans & Wernars, 1991; Chart *et al*., 1998), and results may not agree with DNA-based detection (Notermans & Wernars, 1991). Furthermore, ELISAs for pathogens detection have lower limits ranging from 10^3 to 10^5 cfu per ml. Therefore direct detection of pathogens in foods is not possible and enrichments are required for at least 16 – 24 h. Kits for the detection of bacterial toxins are based mainly on immunoassay systems. Thus, the use of these kits does not give any information on the biological activity of the toxins (Brett, 1998).

3.1.2 *Immunofluorescence assay*

The immunofluorescence assay (IFA) allows the identification and enumeration of a single specific cell in a natural sample (Campbell, 1993). Assays can be performed by a direct or indirect procedure. In a direct immunofluorescence procedure, the specific antibody is directed conjugated with a fluorochrome. An indirect procedure involves the binding of the specific primary antibody to the targeted antigen followed by the addition of a fluorochrome-labelled antibody directly against the first antibody. Nevertheless IFA does not provide information on the physiological status of cells, or on whether they are living or dead (Rompré *et al*., 2002).

3. 2 Microscopy-Based Techniques

As some techniques provide limited information on the number and spatial distribution of micro-organisms, there is a need for a microscopic technique similar to the well-known Gram-staining methods but as sensitive as the immunofluorescence techniques (Bohlool & Schmidt, 1980).

3.2.1 *Direct epifluorescence filter technique (DEFT)*

Fluorescence microscopy has provided a very rapid method for microbial detection and enumeration, and does not require any incubation period. The most successful method of this kind is the direct epifluorescence filters technique (DEFT) (Pettifer *et al*., 1980). This technique uses a membrane filter to isolate cells and takes less than 25 minutes to complete. However, problems are encountered through the interference of particulate matter and the requirement for a long pre-incubation period.

3.2.2 *Fluorescence in situ hybridisation (FISH)*

The FISH technique uses a 'universal' probe for the bacterial domain, potentially allowing the detection of all bacteria present in the sample regardless of their ability to be cultured. FISH with rRNA-targeted oligonucleotide probes has been developed for the *in-situ* identification of microbial cells and is now a well-established technique. It is fully compatible with direct counting methods (Glöckner *et al.*, 1996; Maruyama & Sunamura, 2000). So far, however, microscopic analysis by FISH has not been automated sufficiently to allow high sample throughput, which would be desirable in many ecological investigations (Glöckner *et al*., 1999). Accurate quantification still remains a challenging task. Further development is therefore needed with respect to FISH sensitivity and automation.

3.3 Flow Cytometry

Flow cytometry is a highly effective means for the rapid analysis of individual cells at rates of up to 1000 cells per second. It is conveniently used as a bacterial counter in clinical, environmental, and industrial microbiology (Boye & Lobner-Olesen, 1991; Steen *et al*., 1990). The advantage of flow cytometry lies in its ability to make rapid, quantitative measurements of multiple parameters of each cell within a large number of cells; this makes it possible to define the properties of the overall population and of component subpopulations. However, flow cytometry has been used almost exclusively for measurements on mammalian or at least eukaryotic cells, while they have remained a rarity in microbiology, including bacteriology. The lack of progress in microbiological applications of flow cytometry was the result of several problems encountered when analysing bacteria. The main experimental difficulty in analysing bacteria using flow cytometry is that many of their biological characteristics (including size, shape and DNA content) vary depending upon the growth conditions used, or the source from which the organisms were obtained (Allman *et al*., 1993). Therefore, strict reproducibility of conditions is required in order to produce consistent data. Finally, the capital cost involved in flow cytometry analyses is high which further restricts its use.

3.4 Electrophoresis

Electrophoresis is simply the movement of a charged particle in an electric field. It is a technique used to separate and sometimes purify macromolecules - especially proteins and nucleic acids - that differ in size, charge or conformation (Tiselius, 1937). Depending on the nature of the net charge, the charged particles will migrate either to the cathode or to the anode. Particles can be fractionated on the basis of electrophoretic mobility, which is the ratio of the velocity of a particle in an electric field to the strength of that field (Tiselius, 1937). The electrophoresis techniques that are widely used in biochemistry and molecular biology are gel electrophoresis, capillary electrophoresis and denaturing gradient gel electrophoresis.

3.4.1 *Gel electrophoresis*

Gel electrophoresis is a procedure for separating a mixture of molecules through a stationary material (gel) in an electrical field. Gels have unique electrophoretic properties including a sieving effect that makes their use advantageous for molecular weight based protein and nucleic acid separation (Giddings, 1991). DNA fragments differing by only one base can be separated making it possible to sequence DNA (Trainor, 1990). For very large biopolymer molecules (e.g. DNAs over 30 x 10^6 molecular weight), the polymeric chain orients with the field and snakes (reptates) through the gel. Thus the sieving effect is rendered ineffective. However it can be restored by switching back and forth between fields oriented at different angel. This technique is called pulsed field gel electrophoresis or PFGE (Schwartz & Cantor, 1984).

This technique is tedious and required skilled personnel to operate it. Many factors may affect the quality of electrophoretic separations including instrument assembly, preparation of the gel and sample buffers, gel casting, the nature of the sample and its preparation, and run conditions.

3.4.2 *Capillary electrophoresis*

Capillary electrophoresis (CE) is a method of separating the contaminants and identifying them using retention time. In CE, capillaries are used as the column because, being small, they provide a large area-to-volume ratio which allow for efficient heat dissipation resulting from the high voltage. An ultraviolet detector is used to identify the contaminant and its concentration.

The use of capillary electrophoresis (CE) for the analysis, identification, and characterization of micro-organisms has been gaining in popularity (Boone *et al.*, 1999). The advantages of CE, such as that it requires a small amount of sample, minimal sample preparation, rapid and simultaneous analysis, ease of quantification and identification, and the ability to make viability assessment, make it an attractive technique for the analysis of microbial analytes. Determination of viability and identification of microbes can be accomplished in a single analysis. Fermentation can be monitored using this system. However, the main problem is that it is difficult to express data in concentrations units, because of the low volume load ability of the capillary. Rigorously pre-treatment samples needed to be implemented. Another problem is the presence of particulate matter, which can easily clog the CE system (Veraart *et al*., 1999).

3.4.3 *Denaturing gradient gel electrophoresis*

The usefulness of denaturing gradient gel electrophoresis (DCGE) in the analysis of microbial communities depends on the assumption that different sequences migrate to different positions in DGCE gels. DGCE separates DNA sequences based on their melting behaviour and has been shown to be able to detect differences in the denaturing behaviour of small DNA fragments that differ by as little as one base pair (Jackson *et al*., 2000). In studying microbial communities, one gene, the 16S rRNA gene, is amplified from the extracted DNA from that whole community. This gene is ideal because there is a large database, it is ubiquitous throughout nature, it is rarely laterally transferred (it is species specific) and its function is conserved. This gene is amplified using PCR and then excised and purified. The purified PCR product is then subjected to DGGE, and multiple banding should occur, indicating multiple sequences from the PCR. The ability of the technique to separate genomic sequences differing by more than one base has rarely been examined, although it has been suggested that detection of multiple sequence differences may be more difficult. Indeed, some difficulties have been reported in separating 16S rDNA amplification products from environmental bacteria that were known to be different (Vallaeys *et al*., 1997; Jackson *et al*., 2000). The co-migration of different sequences to the same position shows that the assumption that one band equals one genome is not always valid.

3.5 Impedimetry Methods

The impedimetric instruments are developed for the estimation of microbial population in time. The higher the number of micro-organisms in the fluid indicates the faster the change in the electrical impedance, capacitance (storage of charge at the electrode surface) and conductance (movement of ions between two electrodes). These measurements rely upon the changes of conductivity due mainly to the fact that the microbial catabolism results in the conversion of unchanged substrate molecules to charged metabolites (Arnott *et al*., 1988; Ogden, 1988). This affects the electrical properties of the suspension which caused either (i) changes in electrical conductivity (resistance) in the liquid by the changed product by cells, (ii) changes at the interface of metal electrodes placed into the container of inoculated growth

medium and (iii) changes in the electrical properties of the suspension by the presence of the cells themselves.

There are numbers of established instruments on the market namely, Bactometer (bioMerieux, France), Malthus (Radiometer, Denmark), RABIT (Don Whitley Scientific, UK), Bactrac (Sy-Lab, Austria) and Aber Biomass Monitor (Aber Instrument, UK) that have been introduced. There are differences with respect to the principal systems. The Bactometer instrument has the option of measuring conductance or capacitance, the Malthus measures conductance and the RABIT system is conductance although there is a capacitance component. Whilst the Biomass monitor measures the capacitance of cell suspensions.

Different test types allow the user to select the desired impedance signal, i.e. capacitance, conductance or a combination of these signals.

This method is well suited for the detection of bacteria in clinical specimens, to monitor quality and detect specific food pathogens, also for industrial microbial process control, and for sanitation microbiology. This technique has been used for estimating microbial biomass, for detecting microbial metabolism and for the detecting concentration and physiological state of bacterial. The main disadvantages of impedimetric methods are the lengthy incubation times, 20 – 25 h which are required to achieve a signal corresponding to microbial growth, the high cost of instrumentation and the need for highly trained personnel. In addition, the impedance technique is not suited for testing samples with low numbers of micro-organism.

3.6 Coulter Counter

The Coulter counter manufactured by Coulter Electronic Inc. (Canada) has been widely used to count micro-organisms (Campos *et al*., 2003; De Liguoro *et al*., 2003). It is a device which counts cells as they float in a liquid by passing them through a small aperture that has two electrodes suspended on either side. The device counts whenever a particle goes through the aperture, the electronic system detects a sudden and momentary increase in resistance. The pulse generated by each cell is amplified and recorded electronically, giving a count of the number of the flowing through. However cell concentrations must be kept low for accurate results since high cell densities limit the accuracy occupies the counting aperture. This method is independent of particle shape, colour, and density. In addition, this device is extremely sensitive to invisible air bubbles or anything else that might clog the hole. Furthermore the device can not differentiate between live and dead cell.

3.7 Nucleic Acid-Based Assays

Most of the nucleic acid methods use molecular hybridisation properties, which involve the complementary sequence recognition between the nucleic acid and a nucleic target. A hybridisation reaction can be DNA-DNA hybridisation or DNA-RNA hybridisation. These techniques can be performed within an hour and few days if required cultivation (Rompré *et al*., 2002). The more frequently used nucleic acid-based methods are in-situ hybridisation methods and the amplification techniques.

3.7.1 *Nucleic acid hybridisation*

Nucleic acid hybridisation is typically between a DNA and RNA molecule present in the target organism and a probe DNA which as a sequence complementary to the target sequence. The specificity of a hybridisation assay is controlled by the DNA probe that contains 15 to 10 nucleotides (de Boer & Beumer, 1999). Basically, the steps involve hybridise the cell's nucleic acid with the DNA probe. The formed hybrid is then detected. Among the direct detection techniques use are: (i) labelled DNA probe to hybridise the nucleic acid in the samples and (ii) radioactive or fluorescent probes, while indirect detection is done with enzyme reporters (Barbout & Tice, 1997).

Hybridisation assays for several foodborne pathogens have been commercialised. The Gene-Trak System (Neogen, USA) uses pathogen-specific probes for ribosomal RNA targets in the bacteria and a colorimetric system for detecting the specific probe-target hybrids. However enrichment is necessary to obtain the required sensitivity (de Boer & Beumer, 1999).

3.7.2 *Amplification Methods*

The more frequently used amplification method is the polymerase chain reaction (PCR). PCR allows a DNA target fragment to be amplified by cycling replication. Detection specificity depends on the degree of homology and complementary between target and primer and on hybridisation temperature. The PCR method has often been described for the detection and identification of micro-organisms in foods, soils, sediments and waters (Trevors & van Elsas, 1995).

PCR has distinct advantages of specificity, sensitivity, rapidity, accuracy and capacity to detect small amounts of target nucleic acid in a sample. PCR has been shown to accurately detect low numbers of microbes such as viruses, bacteria, protozoa and helminthes and multiple primers can be used to detect different pathogens in one multiplex. Despite its sensitivity, it is difficult to use PCR for quantification of micro-organisms.

Problems such as the sensitivity of the polymerase enzyme to environmental contaminants, difficulties in quantification, the generation of false positives through in quantification, the generation of non-viable micro-organisms or contamination of samples in the laboratory, may limit the use of PCR for the direct detection of microbial contamination. In addition, the PCR method cannot differentiate DNA from dead and living microorganisms or contaminating DNA from previous amplicons.

3.7.3 *DNA microarrays*

Recently, the invention of the DNA microarrays has provided a simple and natural vehicle for exploring the genome in a way that is both systematic and comprehensive (Wodicka *et al*., 1997; Lashkari *et al*., 1997). It is a powerful tool for analysis of RNA or DNA composition on a whole-genome scale. Two systems are used, one in which short oligonucleotides have been synthesised directly on the solid support (Chee *et al*., 1996) and one in which short DNA molecules are synthesised and then fixed on a suitable support using robotics (Shena, 1996).

DNA microarrays have a significant impact in understanding normal and abnormal cell biochemistry and thus are the choice of targets for drug design. However, their use has not been restricted to human cell biology. DNA microrrays also can be used for the identification of bacteria in a mixture: the DNA or cDNA from an entire bacterial population can be isolated and hybridised to an array of 16S ribosomal DNA fragments giving information on both abundance and identity of bacteria in a particular environment.

The use of microarrays to monitor gene expression is a rapidly evolving technology that continues to gain momentum. However, because of its expense and because it is complicated, requiring highly skilled workers to carry out tests, its immediate role will probably be restricted to infections where the causative organism cannot be cultured or is difficult to detect by conventional means.

Table 2 summarises the general advantages and disadvantages of DNA-based methods.

Table 2. A summary of general advantages and problems of DNA-based methods for detection and characterisation of pathogens compared to traditional culture based methods (adapted from Olsen, 2000)

Application	Advantages	Problems
Direct detection of pathogens	Does not (in theory) require cultivation	May detect dead cells (PCR) High detection level due to small test volume Inhibition due to surrounding components (PCR). Very sensitive to laboratory contamination (PCR)
Culture confirmation on enrichment media	Rapid and sensitive Automatic detection possible Insensitive to high concentrations of indigenous microbiota	No colony obtained, and hence most suitable for screening out negative samples.
Characterisation of pathogenic bacteria from samples	Can separate virulent from non-virulent bacteria by targeting virulence genes Multiplex characterisation possible (PCR)	
Other applications	Can specifically detect genetically modified organisms.	

3.8 Fatty Acid Based Technique

The fatty acid methyl ester (FAME) analysis is widely used for the identification of micro-organisms. It compares the differences of the type and the distribution of fatty acids in microbial communities. Fatty acids are found in all living organisms with cell membranes. Analyses of gases produced from the bacteria have been used to identify bacteria and other pathogens at the genus level, and often at the species level. The fatty acids are extracted from the bacteria to be identified, made volatile by methyl esterification, and subjected to chromatography. The resultant chromatogram yields a profile pattern that is analysed statistically to identify the bacteria. The specific phospholipids and their abundance depend on the particular organism and are sufficiently distinctive for the identification of isolated pure cultures (Lechevalier, 1977; Sasser, 1990). FAME analysis has been used as biochemical characters to study many different groups of organisms such as bacteria and fungi. However, results can be variable and are highly dependent on the culture conditions and temperature used. Additionally, standard techniques involve microbial culture, usually for 24 hours and a lengthy extraction/derivatisation step before analysis by chromatography, and the instrumentation is costly.

3.9 Mass Spectrometry

Mass spectrometry used the separation of matter according to their mass-to-charge ratio. It relies on the production of ions from a sample compound and the subsequent characterisation of the patents that are produced. It is a powerful tool to be used in identification and detection of materials compound in

sample, pathogens or aiding cancer diagnosis. Continuous development and improvement of instrumentation and techniques have made mass spectrometry the most versatile, sensitive and widely used analytical method available today. Because of its great sensitivity and ability to identify chemical compounds positively, it can be coupled with other methods such as gas chromatography (GC), liquid chromatography (LC), capillary electrophoresis (CE) and supercritical fluid chromatography (Careri et al., 2002). A useful overview of mass spectrometry (MS) may be found at the website of the American Society for Mass Spectrometry: www.asms.org/whatisms.

Over the past decade, the mass range and sensitivity of the instrumentation have been developed intensively. Today, GC-MS, LC-MS, Tandem MS (MS-MS), electrospray ionisation (ESI-MS), matrix-assisted laser desorption/ionisation (MALDI-MS), and inductively coupled plasma (ICP-MS) are commonly used as analytical tool.

More specifically, electrospray ionisation (ESI) and MALDI, have had significant impact on the capabilities of mass spectrometry. Both ESI and MALDI have allowed for sophisticated applications of mass spectrometry to the field of biology and medicine. The limitations of mass spectrometry have yet to be defined as larger and more complex molecules are being successfully characterised. Applications that were once inconceivable are in wide used today include: sequencing of peptides and proteins; studies of non-covalent complexes and immunological molecules; DNA sequencing; and the analysis of intact viruses. In the 1990's, mass spectrometry hit the mainstream chemistry and biochemistry laboratories with commercially available, high performance instruments.

Liquid chromatography-mass spectrometry (LC-MS) coupling has led to the development of new interfaces, extending the possibilities and automation of various procedures even more. Significant advances in ionisation techniques having a broad range of applicability and high sensitivity for the analysis of high-polar and high molecular mass compounds of sample have been the key of this development in the last years. In recent years, ICP-MS coupled with LC has become an analytical technique with many applications in the study, for example in food analysis and in the specified of inorganic and organometallic compounds.

Varying amounts of sequence information can be obtained from each fragmentation spectrum, and the spectra need to be interpreted carefully. Some of the processing can be automated, but in general the processing and interpretation of spectra will take longer than the data acquisition if accurate and reliable data are to be generated. This technique is not easy to handle as it requires skilled personnel. And furthermore, the instrumentation is costly.

4. SUMMARY

Although there are numerous products available which are able to deliver low detection limits within hours for a wide range of samples, there is still a need for a microbial detector which can provide a sensitivity of 10^2 - 10^3 cells ml^{-1}, with a rapid analysis time at a relatively low cost.

In general, individual methods suffer from various disadvantages that include a lengthy analysis time, high cost of instrument and lack of sensitivity. Many methods are not suitable for industrial application due to the interfering characteristics of bioprocesses.

REFERENCES

Adams, J. C., Lytle, M. S., Dickman, D. G., Foster, D. H., Connell, J. P. & Bressler, W. R. (1989). Comparisation of methods for enumaeration of selected coliforms exposed to ozone. *Appl. Environ. Microbiol.*, **55**: 33-35.

AFNOR (Association Française de Normalisation) (1990). Eauc-méthodes d'essais. Recueil de Normes Françaises. 4th edn. Ia Défense, Paris, pp. 735.

APHA, AWWA, AEF (1998). Standard Methods for the Examination of Water and Wastewater, 20th edn. Washington, DC.

Allman, R., Manchee, R. & Lloyd, D. (1993). Flow cytometric analysis of heterogeneous bacterial populatons. *In* Flow Cytometry in Microbiology. Lloyd, D. (Ed.) Springer-Verlag London Limited, Germany, pp. 27 – 47.

Arnott, M. L., Gutterige, C. S., Pugh, J. S. & Griffits, J. L. (1988). Detection of *Salmonella* in confectionary products by conductance. *J. Appl. Bacteriol*., **64**: 409-420.

Barbour, W. M. & Tice, G. (1997). Genetic and immunologic techniques for the detecting foodborne pathogens and toxins. In *Food Microbiology*. Doyle, M. P., Beuchat, L. R. & Montville, T. J. (Eds.). Fundamentals and Frontiers, ASM Press, Washington DC, pp. 710-727.

Basile, F., Beverly, M. B. & Voorhees, K. J. (1998). Pathogenic bacteria: the detection and differentiation by rapid lipid profiling with pyrolysis mass-spectrometry. *Trends Anal. Chem*., **17**: 95-109.

Begot, C., Desnier, I., Daudin, J. D., Labadie, J. C. & Lebert, A. (1996). Recommendations for calculating growth parameters by optical density measurements. *J. Microbiol. Methods*, **25**: 225-232.

Bohlool, B. B. & Schmidt, E. L. (1980). The immunofluorescence approach in microbial ecology. *Adv. Microb. Ecol.*, **4**: 203-241.

Boone, C. M., Waterval, J. C. M., Lingerman, H., Ensing, K. & Underberg, W. J. M. (1999). Capillary electrophoresis as a versatile tool for the bioanalysis of drugs – a review. *J. Pharmaceu. Biomed. Anal*., **20**: 831-863.

Boye, E. & Lobner-Olesen, A. (1991). Bacterial growth control studied by flow cytometry. *Res. Microbiol*., **142**: 131-135.

Brett, M. M. (1998). Kits for the detection of some food poisoning toxins: problems, pitfalls and benefits. *J. Appl. Microbiol. Symp. Suppl*., **84:** 110S – 118S.

Burlingame, G. A., McElhaney, J., Bennett, M. & Pipes, W. O. (1984). Bacteria interference with coliform colony sheen production on membrane filters. *Appl. Environ. Microbiol*., **47**: 56-60.

Campbell, L. (1993). Immunofluorescence method for the detection and characterization of marine microbes. In Handbook of Methods in Aquatic Microbial Ecology. Kemp, P. F., Sherr, B. F. & Cole, J. J. (Eds). Lewis Publishers, Boca Raton, FL, USA, pp. 3558-3564.

Campos, J. A., Aledo, J. C., Segura, J. A., Alonso, F. J. & Gómez, P. M. (2003). Expression of recombinant human-glutaminase in *Escherichia coli*: polyclonal antibodies production and immunological analysis of mouse tissues. *BBA - Proteins & Proteomics*, **1648***:* 17-23.

Chee, M., Yang, R., Hubble, E., Berno, A., Huang, X. C., Stern, D., Winkler, J., Lockhart, D. J., Morris, M. S. & Fodor, S. P. (1996). Accessing genetic information with high-density DNA-arrays. *Science*, **273**: 610-614.

Cox, G. (2000). Biological confocal microscopy. *Materials Today*. March, p: 34 – 41.

de Boer, N. & Beumer, R. R. (1999). Methodology for detection and typing of foodborne microorganisms. *Intl. J. Food Microbiol*., **50**: 119-130.

De Liguoro, M., Cibin, V., Capolongo, F., Halling-Sorensen, B. & Montesissa, C. (2003). Use of oxytetracycline and tylosin in intensive calf farming: evaluation of transfer to manure and soil. *Chemosphere*, **52**: 203-212

Clark, J. A. (1980). The influence of inceasing numbers of non-indicator organisms by the membrane filter and presence – absence test. *Can. J. Microbiol*., 26: 827.

Evans, T. M., Waarvick., C. E., Seidler, R. J. & LeChevallier, M. W. (1981). Failure of the most-probable-number technique to detect coliforms in drinking water and raw water supplies. *Appl. Environ. Microbiol*., **41**: 130-138.

Fung, D. Y. C. (1995). What's needed in rapid detection of foodborne pathogens. *Food Technol*., **49**: 64-67.

Giddings, J. C. (1991). Unified Separation Science, Wiley, New York.

Glöckner, F. O., Amann, R., Alfreider, A., Pernthaler, J., Psenner, R., Trebesius, K. & Schleifer, K-H. (1996). An *in situ* hybridisation protocol for detection and identification of planktonik bacteria. *Sys. Appl. Microbiol*., **19**: 403-406.

Glöckner, F. O., Fuchs, B. M. & Amann, R. (1999). Bacterioplankton composition in lakes and oceans: a first comparison based on fluorescence in situ hybridisation. *Appl. Environ. Microbiol*., **65**: 3721-3726.

Hobson, N. S., Tothill, I. & Turner, A. P. F. (1996). Microbial detection. *Biosensors Bioelectron*., **11**: 455-477.

Hsu, S. C. & Williams, T. J. (1982). Evaluations of factors affecting the membrane filter technique for testing drinking water. *Appl. Environ. Microbiol*., **44**: 453-460.

Hübner, I., Steinmetz, I., Obst, U., Giebel, D. & Bitter-Suermann, D. (1992). Rapid determination of members of the family *Enterobacteriaceae* in drinking water by an immunological assay using a monoclonal antibody against enterobacterial common antigens. *Appl. Environ. Microbiol*., **58**: 3187-3191.

Jackson, C. R., Roden, E. E. & Churchill, P. F. (2000). Denaturing gradient gel electrophoresis can fail to separate 16S rDNA fragments with multiple base differences. *Molecular Biol. Today*, **1**: 49-51

Jones, A. M. & Knowles, R. (1991). Enumeration of Flexibacter Canadensis in environmental samples by using a bacteriophage isolated from soil. *Appl. Environ. Microbiol*., **57**: 3043-3045.

Kemeny, K. M. (1991). *In* A Practical Guide to ELISA. NY, Pergamon Press.

Lashkari, D., DeRisi, J., McCusker, J., Namath, A., Gentile, C., Hwang, S., Brown, P. & Davis, R. (1997) Yeast genome microarrays for parallel genetic and gene expression analysis of the yeast genome. *Proc. Natl Acad. Sci. USA*, **94**: 13057-13062.

Lechevalier, M. P. (1977). Lipids in bacterial taxonomy – A taxonomist's view. *Crit. Rev. Microbiol.,* **5**: 109-210.

Little, B., Staehleb, R. & Davis, R. (2001). Fungal influenced corrosion of post-tensioned cables. *Inter. Biodeterioration & Biodegradation*, **47**: 71-77.

Manafi, M. (1996). Fluorogenic and chromogenic substrates in culture media and identification tests. *Intl. J. Food Microbiol.* **31**: 45-48.

Märtlbauer, E. & Becker, H. (1995). Immunologischer Nachweis von Mikroorganismen und Toxinen Lebensmitteln: Anwendungen und Perspektiven. *Fleischwirtschaft,* **75**: 1092 – 1098.

Maruyama, A. & Sunamura, M. (2000). Simultaneous direct counting of total and specific microbial cells in seawater, using a deep-sea microbe as target. *Appl. Environ. Microbiol*., **66**: 2211-2215.

McFeters, G. A., Cameron, S. C. & LeChevallier, M. W. (1982). Influence of diluents, media and membrane filters on detection of injured waterborne coliform bacteria. *Appl. Environ. Microbiol.*, **43**: 97-103.

McMeekin, T. A., Olley, J. N., Ross, T. & Ratkowsky, D. A. (1993). Optical density methods. *In* Predictive Microbiology. Wiley, Chister, U.K., pp. 31-34.

Means, E. G. & Olson, B. H. (1981). Coliform inhibition by bacteriocin-like substances in drinking water distribution systems. *Appl. Environ. Microbiol*., **42**: 506-512.

Metcalf, T. G., Melnick, J. L. & Estes, M. K. (1995). Environmental virology: from detection of virus in sewage and water by isolation to identification the molecular biology – a trip of over 50 years. *Ann. Rev. Microbiol*., **49**: 461-487.

Neu, T.R. & Lawrence, J.R. (1997). Development and structure of microbial biofilms in river water studied by confocal laser scanning microscopy. *FEMS Microbiol. Ecol.*, **24**: 11-25.

Niskanen, A. & Aalto, M. (1978). Comparison of selective media for coagulase-positive enterotoxigenic *Staphylococcus aureus*. *Appl. Environ. Microbiol.*, **35**: 1233-1236.

Noleto, A. L. & Bergdoll, M. S. (1980). Staphylococcal enterotoxin production in the presence of non-enterotoxigenic staphylococci. *Appl. Environ. Microbiol*., **39**: 1167-1171.

Notermans, S. & Wernars, K. (1991). Immunological methods for detection of foodborne pathogens and their toxins. *Intl. J. Food Microbiol*., **12**: 91-102.

Nybroe, O., Johansen, A. & Laake, M. (1990). Enzyme-linked immunosorbent assays for detection of Pseudomonas fluorescens in sediment samples. *Lett. Appl. Microbiol*., **11**: 293-296.
Ogden, I. D. (1988). A conductance medium to distinguish between *Salmonella* and *Cytrobacter* spp. *Int. J. Food. Microbiol*., **7**: 287-297.
Olsen, J. E. (2000). DNA-based methods for detection of food-borne bacterial pathogens. *Food Res. Intl*., **33**: 257-266.
Perez, F. G., Muscini, M., Tothill, I. E. & Turner, A. P. F. (1998). Immunomagnetic separation with mediated flow-injection analysis amperometric detection of viable *E. coli* 0157:H7. *Anal. Chem*. **70**: 2380-2386.
Peterz, M. & Steneryd, A. C. (1993). Freeze-dried mixed cultures as reference samples in quantitative and qualitative microbiological examinations of food. *J. Appl. Bacteriol*., **74**: 143-148.
Pettifer, G. L., Mansell, R., McKinnon, C. H. & Cousins, C. N. (1980). Rapid membrane filtration epifluorescence microscopy technique for the direct enumeration of bacteria in raw milk. *J. Appl. Environ. Microbiol*., **29**: 29-31.
Pósfaia, M., Lib, J., Andersonc, J. R. & Buseck, P. R. (2003). Aerosol bacterial over the Southern Ocean during ACE-1. *Atmospheric Res*., **66**: 231-240.
Rayman, K., Malik, N. & Jarvis, G. (1998). Performance of four selective media for enumerating *Staphylococcus aureus* in corned beef and cheese. *J. Food Prot*., **51**: 87-88.
Rice, E. W., Fox, K. R., Read, E. J. & Smith, A. P. (1987). Comparison of media for recovery of total coliform bacteria from chemically treated water. *Appl. Environ. Microbiol*., **53**: 1571-1573.
Rompré, A., Servais, P., Baudart, J., de-Roubin, M-R. & Laurent, P. (2002). Detection and enumeration of coliforms in drinking water: cuurent methods and emerging approaches. *J. Microbiol. Methods*, **49**: 31-54.
Sasser, M. (1990). Identification of bacteria through fatty acid analysis. *In* Methods in Phytobacteriology. Z. Klement *et al*. (eds.), Adademiai, Kiado, Budapest. pp. 199-204.
Steen, H. B., Skaratad, K. & Boye, E. (1990). DNA measurement of bacteria. *In* Methods in Cell Biology, vol. 33, Darzynkiewicz, Z. & Crissman, H. (Eds.). Academic Press, San Diego, pp. 519-526.
Shena, M. (1996). Genome analysis with gene expression microrrays. *BioEssays*, **18:** 98-102.
Schwartz, D. C. & Cantor, C. R. (1984). Separation of yeast chromosome-sized DNAs by pulsed field gradient gel electrophoresis. *Cell*, **37**: 67-75.
Tiselius, A. (1937). A new apparatus for electrophoretic analysis of colloidal mixtures. *Trans. Faraday Soc*., **33**: 524.
Tietjen, M. & Fung, D. Y. C. (1995). *Salmonella* and food safety. *Crit. Rev. Microb*., **21**: 53-83.
Trainor, G. L. (1990). DNA sequencing, automation, and the human genome. *Anal Chem*., **62**: 418-426.
Tsen, H. Y., Lin, C. K. & Chi, W. R. (1998). Development and use of 16S rRNA gene targeted PCR primer for the identification of *Escherichia coli* in water. *J. Appl. Microbiol*., **61**: 554-560.
Vallaeys, T., Topp, E., Muyzer, G., Macheret, V., Languerre, G., Rigaud, A. & Soulas, G. (1997). Evaluation of denaturing gradient gel electrophoresis in the detection of 16S rDNA sequence variation in rhizobia and methanotrophs. *FEMS Microbiol. Ecol*., **24**: 279-285.
Veraat, J. R., Lingerman, H. & Brinkman, U. A. Th. (1999). Coupling of biological sample handling and capillary electrophoresis. *J. Chromatography A,* **856**: 483-514.
Westall, F., de Witb, M. J., Dannb, J., van der Gaastc, S., de Ronded, C. E. J. & Gerneke, D. (2001). Early Archean fossil bacteria and biofilms in hydrothermally-influenced sediments from the Barberton greenstone belt, South Africa. *Precambrian Res*., **106**: 93-116.
Wodicka, L., Dong, H., Mittmann, M., Ho, M. H. & Lockhart, D. J. (1997). Genome-wide expression monitoring in *Saccharomyces cerevisiae*. *Nat. Biotechnol*., **15**: 1359-1367.

DEVELOPMENT AND VALIDATION OF SOFTWARE TOOLS FOR WCDMA COVERAGE PREDICTION

Rafidah bt Abd Malik

Instrumentation & Electronic Technology Division, STRIDE
Taman Bukit Mewah Fasa 9, 43000 Kajang, Selangor D.E.
Tel: 03-87324440
Fax: 03-87348695
E-mail: rafasa04@gmail.com

Abstract

Nowadays the propagation model is a very important component in coverage planning of cellular radio systems. Therefore software tools have been developed to predict average signal strengths and path loss signal in urban area of Wideband Code Division Multiple Access (WCDMA) system. In this paper, empirical and semi-deterministic propagation models have been used as basis to analyse coverage prediction using test drive data obtained from the field. Calculations of error measurements enable users to find a minimum error between calculated signal strength and actual signal strength data. Moreover, accuracy of actual data has been validated through error measurement. Modified propagation models are then used to predict new coverage area in selected area.

Keywords: *Propagation model; Urban area; WCDMA system; Signal strength; Error measurement; coverage prediction.*

1. INTRODUCTION

Third Generation Mobile Radio (3G) technology that used Wideband Code Division Multiple Access (WCDMA) as its air-interface has set new requirements to radio network planning. WCDMA radio network planning is closely related to the optimization of radio network. The planning of 3G system is very different from 2G such as GSM which adopts a time division multiple access technology (TDMA).

The efficient network planning is a vital aspect of 3G networks, and key differences arise between 2G and 3G networks due to the different level of service offered (Guo *et al*., 2003). Reason of network planning is to maximise the coverage, capacity, cost and the quality of service. The planning process aims to allow the maximum number of users sending and receiving adequate signal strength in a cell.

There is a need to study the techniques used in WCDMA in the radio network planning process and how to optimise the WCDMA performance especially for a better coverage (Ching, 2006). In this research, only coverage planning will be considered. This will be done by performing the coverage prediction using propagation models.

Three well-known propagation models for urban area have been used as basis to analyse coverage prediction using signal strength obtained from collected test drive measurement. The use of precise path loss model for coverage prediction is essential for a cellular radio network operator to plan transmitter installations, cellular network optimisation for interference analysis and growth plan (Kandasamy, *et al*., 2004).

2. THEORETICAL ANALYSIS

Empirical and semi-deterministic propagation models have been studied in this research. Modified Okumura Hata (MOH), Extended COST 231 (COST-231) and COST 231 Walficsh-Ikegami (COST231-WI) propagation models have been proposed to predict a coverage area in urban environment.

2.1 MOH

The MOH path loss, L_{MOH} model is given by Maciej *et al.* (2006):

$$L_{MOH} = A + B \log_{10}(R) - a(hm) \quad \text{(dB)} \tag{1}$$

where $A = 46.3 + 33.9 \log_{10}(fc) + 10\log_{10}(fc/2000 - 13.82 \log_{10}(h_{tx})$ (2)

$B = 44.9 - 6.55 \log_{10}(h_{tx})$ (3)

$a(hm) =$ correction factor

$= 3.2 (\log_{10}(11.7554(h_{rx})))^2 - 4.97 - 20\log_{10}(h_{tx}/30)$ (4)

Furthermore, fc is the downlink frequency, h_{tx} is the antenna height of base station and h_{rx} is the antenna height of mobile station.

2.2 COST-231

The COST-231 path loss, $L_{COST231}$ model is given by Casaravilla *et al*. (2003) and Zreikat & Al-Begain (2003):

$$L_{COST231} = A + B\log_{10}(R) - a(hm) + G \quad \text{(dB)} \tag{5}$$

where $A = 46.3 + 33.9\log_{10}(fc) - 13.82\log_{10}(h_{tx})$ (6)

B is defined in equation (3)

$a(hm) = (1.1 \log_{10}(fc) - 0.7)\, hm - (1.56 \log_{10}(fc) - 0.8)$ (7)

$$G = \begin{cases} 0 \text{ dB for medium sized city and} \\ \text{suburban centres with medium tree density} \\ 3 \text{ dB for metropolitan centres} \end{cases} \tag{8}$$

2.3 COST231-WI

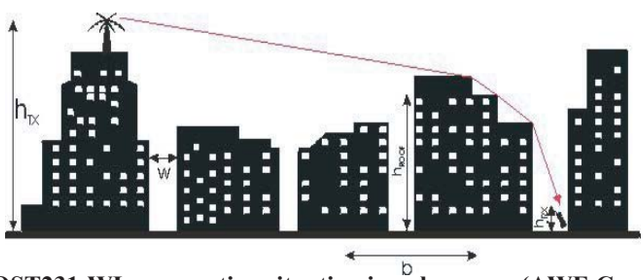

Figure 1: COST231-WI propagation situation in urban area (AWE Communications Software Development, 2003)

COST231-WI has been adopted as a standard model for 3G IMT 2000/UMTS systems [4]. This model distinguishes between line-of-sight (LOS) and non-line-of-sight (NLOS) situations. The formulation of the LOS model is given by (Nawrocki *et al*., 2006) and Casaravilla *et al*. (2003):

$$LOS_{COST\text{-}WI} = 42.6 + 26\ log_{10}(R) + 20log_{10}(fc)\ \text{(dB)} \quad (9)$$

If a NLOS exists, path loss defined by (Nawrocki *et al*., 2006):

$$L_{COST\text{-}WI} = L_{FS} + L_{rts} + L_{MSD}\ \text{(dB)} \quad (10)$$

where L_{FS} = free space path loss

$$= 32.45 + 20log_{10}(R) + 20log_{10}(fc) \quad (11)$$

L_{rts} = roof-to-street loss

$$= -16.9 + 10log_{10}(fc) + 20log_{10}(\Delta h_{rx}) - 10\ log_{10}(w) + L_{ori} \quad (12)$$

L_{ori} = street orientation function

$$L_{ori} = \begin{cases} -10 + 0.354\ \Phi & 0 \le \Phi < 35° \\ 2.5 + 0.075\ (\Phi - 35) & 35° \le \Phi < 55° \\ 4.0 - 0.114\ (\Phi - 55) & 55° \le \Phi < 90° \end{cases} \quad (13)$$

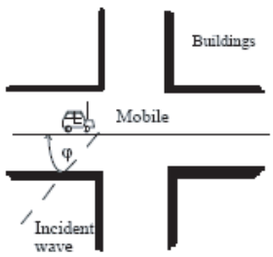

Figure 2: Definition of Street Orientation Angle, Φ (Lempiäinen *et al*., 2001)

L_{MSD} = multi-diffraction loss

$$= L_{bsh} + ka + kdlog_{10}(R) + kflog10(fc) - 9\ log10(b) \quad (14)$$

where $L_{bsh} = \begin{cases} -18\ log10\ (1 + \Delta h_{tx}) & \text{for } h_{tx} > h_{Roof} \\ 0 & \text{for } h_{tx} \le h_{Roof} \end{cases}$ (15)

with h_{Roof} is the height of building, b is the building separation, w is the road width and Φ is the road orientation as shown in Figure 2.

$$ka = \begin{cases} 54 & h_{tx} > h_{Roof} \\ 54 - 0.8\ \Delta h_{tx} \text{ for } R \ge 0.5 \text{ km and} & h_{tx} \le h_{Roof} \\ 54 - 0.8\ \Delta h_{tx}(R)/0.5 \text{ for } R < 0.5 \text{ km} & h_{tx} \le h_{Roof} \end{cases} \quad (16)$$

$$kd = \begin{cases} 18 & h_{tx} > h_{Roof} \\ 18 - 15\ \Delta h_{tx} / h_{Roof} & h_{tx} \le h_{Roof} \end{cases} \quad (17)$$

$$kf = \begin{cases} -4 + 0.7\ (f / 925 - 1) \text{ medium sized city} \\ 1.5\ (f / 925 - 1) \text{ metropolitan center} \end{cases} \quad (18)$$

Δh_{rx} = difference between h_{Roof} and h_{rx}

$$= h_{Roof} - h_{rx} \quad (19)$$

Δh_{tx} = difference between h_{tx} and h_{Roof}

$$= h_{tx} - h_{Roof} \quad (20)$$

3. COVERAGE PREDICTION

3.1 Urban Coverage Area

Putrajaya and Cyberjaya areas have been selected as coverage area. These areas represent urban environment. From digital map as illustrated in Figure 3, the coverage area is 11.20 km × 11.12 km wide. Thus the size of prediction area is 11.20 km × 11.12 km = 124.544 km^2. Longitude (x) and latitude (y) for this area are x axis; 101.63 to 101.73 and y axis; 2.88 to 2.98.

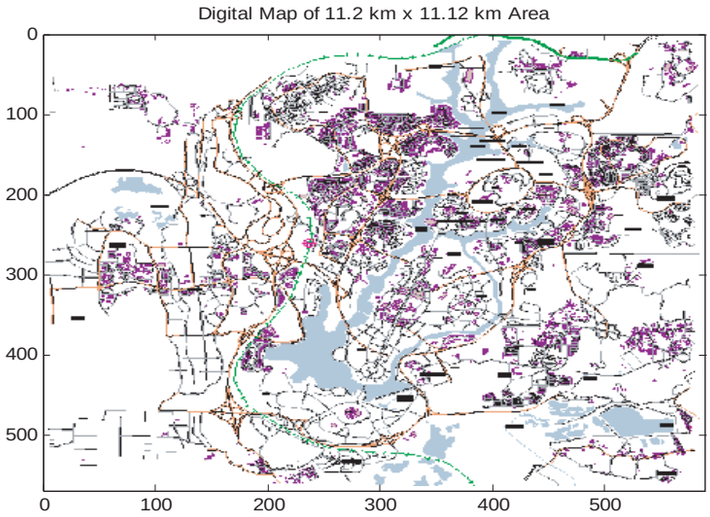

Figure 3: Figure 4.6: Putrajaya and Cyberjaya in area 11.20 km x 11.12 km wide

3.2 Base station and Mobile station

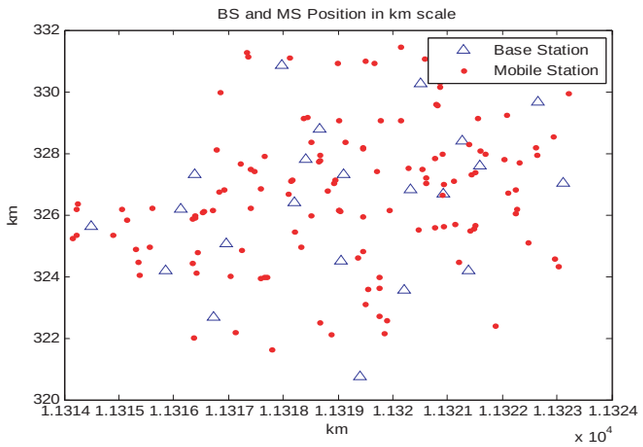

Figure 4: Position of base stations and mobile stations in kilometer

Actual data of base stations and mobile stations position have been plotted in one graph. Meanwhile distance between mobile stations and base stations have been calculated through MATLAB programmed. The position of mobile stations and base stations in kilometer scale is shown in Figure 4. This is the coverage threshold for predicting the coverage area. Actual signal strength for tests drive data is known as received signal strength indicator (RSSI). RSSI is the threshold values for predicted signal strength at selected area.

4. Modelling and Simulation

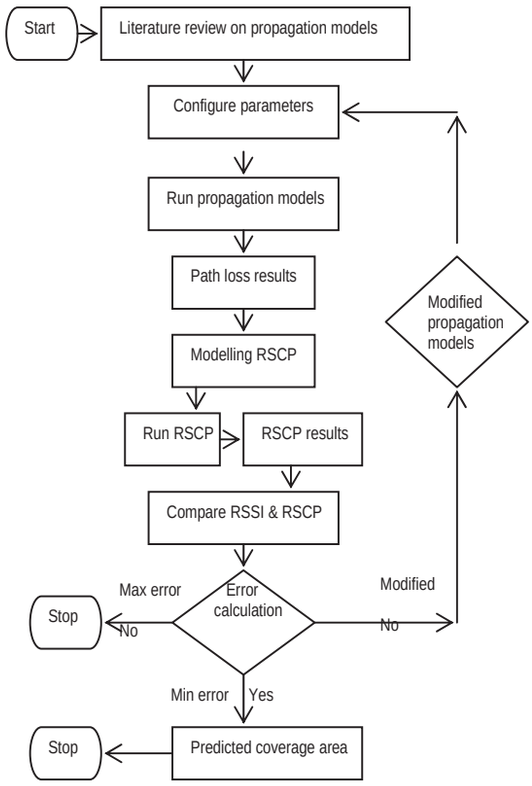

Figure 5: Configuration and Simulation Flow Chart

The modelling of received signal common power (RSCP) or *Pr* is described in equation (21). This signal strength is called RSCP because it received power from common pilot channel (CPICH) of base station. Parameters involved in propagation models, *L* and *Pr* are listed in Table 1 and 2. Overall process of coverage prediction has been revealed in Figure 5.

$$Pr = Pt + Gt + Gr - L - Losses + Fading \ \text{(dBm)} \quad (21)$$

Table 1: Default parameters for Modified Okumura-Hata, COST231 and COST-WI

Parameters	MOH	COST 231	COST-WI
fc	2100 MHz	2100 MHz	2100 MHz
h_{tx}	30 m	30 m	30 m
h_{rx}	1.5 m	1.5 m	1.5 m
h_{Roof}	-	-	30 m
w	-	-	25 m
b	-	-	50 m
phi (Φ)	-	-	90°

Table 2: Default parameters for Modelling RSCP

Parameters	Pr = Pt + Gt + Gr – Lp – Losses + Gain + Fading
Pt (CPICH)	33 dBm
Gt	18 dBi
Gr	0 dBi
Losses	3 dB
Gain	4.1 dB
Fading	Rayleigh Channel

5. PERFORMANCE ANALYSIS

5.1 RSSI compared with three RSCP

When all the signal strength have been plotted in single graph as in Figure 6, it shows that values or behaviour of RSCP signal for MOH and COTS-231 is parallel. This occurrence has been explained in (www.ee.bilkent.edu.tr), i.e. path loss for Cost-231 shows similar manners with MOH in urban area.

Meanwhile for COST231-WI is left far behind from the actual values. However COST231-WI propagation model can still be modified because in modelling, antenna height of base station is the same level with building height i.e. 30 m. As highlighted in Nawrocki *et al*. (2006) and Matha (1999), to get better results of RSCP values for COST231-WI, height of antenna base station should be mounted above medium rooftop level.

5.2 Error Measurement and Validation of Software tools

Error measurements for three propagation models have been calculated as given by:

$$E1 = RSSI - Pr_{MOH} \quad (22)$$

$$E2 = RSSI - Pr_{COST231} \quad (23)$$

$$E3 = RSSI - Pr_{COST\text{-}WI} \quad (24)$$

Minimum and maximum values of errors have been recognised by measurement and empirical cumulative distribution function (cdf) plot as illustrated in Figure 7. Therefore which propagation models are suited for WCDMA at urban area would be identified. Consequently, RSCP from software tools is also validated by error measurement.

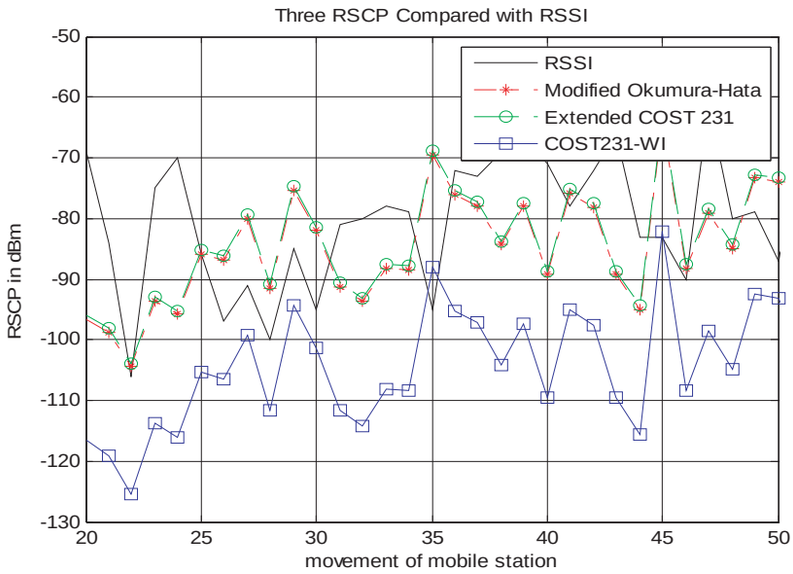

Figure 6: Plotted graph for RSSI and three RSCP

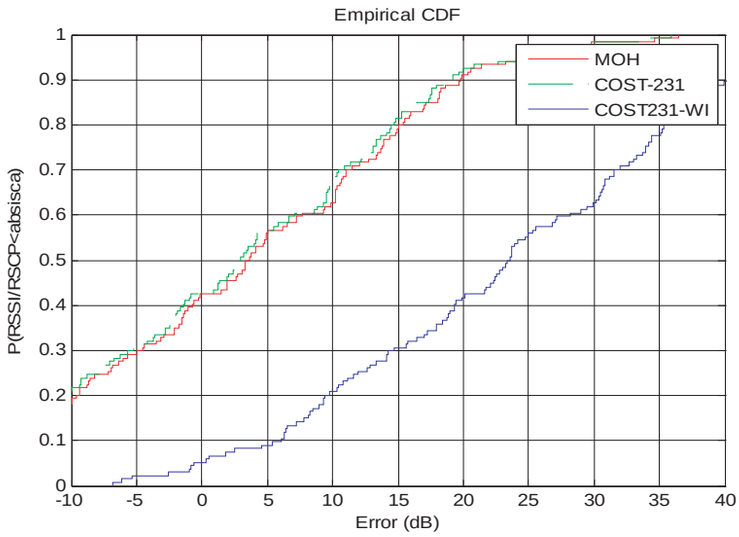

Figure 7: Cdf plot of error measurement (before modification)

Observation from the graph shows values of median error for COST231-WI is the worst and COST-231 is the best, as shown in Table 3. However propagation models that have maximum error or potential to be repaired can be modified to obtain better error, i.e. approximately to zero value. A parameter that has been adjusted to get better result is antenna height of base station, h_{tx}.

Table 3: Median error values for Three Propagation Models

Propagation Models	Median Error
Modified Okumura-Hata	3.4868
COST-231	2.8371
COST231-WI	23.4416

5.3 Modified Propagation Model

Once h_{tx} is changed to 49 m, just two propagation models can be modified, that is COST-231 and COST231-WI. While applying this value to COST-231 and COST231-WI propagation models, values of median error for these models are close to 0 dB. The deflation of COST-231 is 2.81 and for COST231-WI is 23.42 compared to before. As explained in Table 4, median error for COST231-WI is 0.8 % better than COST-231.

Table 4: Median error values for Modified Propagation Models

Propagation Models	Median Error
COST-231	0.0311
COST231-WI	0.0231

This indicates that both propagation models are suitable to be applied in urban environment. However, COST231-WI is more suitable in urban area as mentioned in Nawrocki *et al*. (2006). Figure 8 is the new cdf plot for modified propagation models.

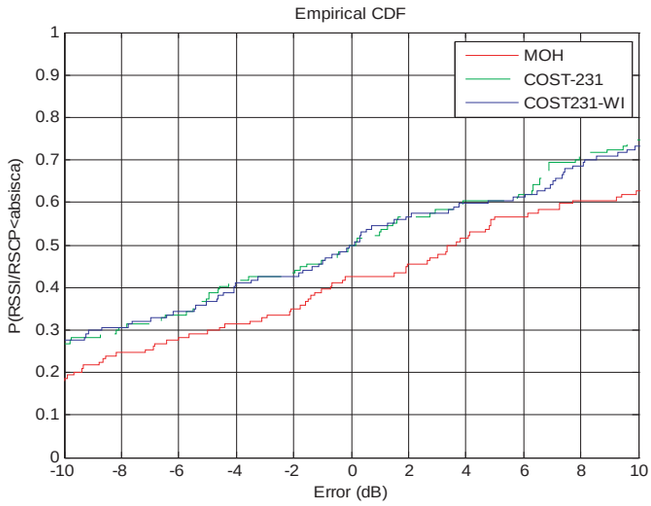

Figure 8: Cdf plot of error measurement (after modification)

5.4 Predicted Coverage Area

Better propagation models have been created after a slight parameter adjustment. From this modified propagation models, new coverage area for WCDMA network in Putrajaya and Cyberjaya area can be predicted. The movements of mobile stations have been set up to 100 positions or samples.

a) Default Base Station Position

Figure 9 is the predicted coverage area for COST-231 and Figure 10 is the predicted coverage area for COST231-WI. From a contour plot, coverage areas from different RSCP levels have been identified. A first six levels are the good RSCP value, i.e. -85 dBm and above. By simulation, the good RSCP value for COST-231 is 67.59 % and for COST231-WI is 65.13 %. These results show the software tools is able to plot the coverage area at Putrajaya and Cyberjaya.

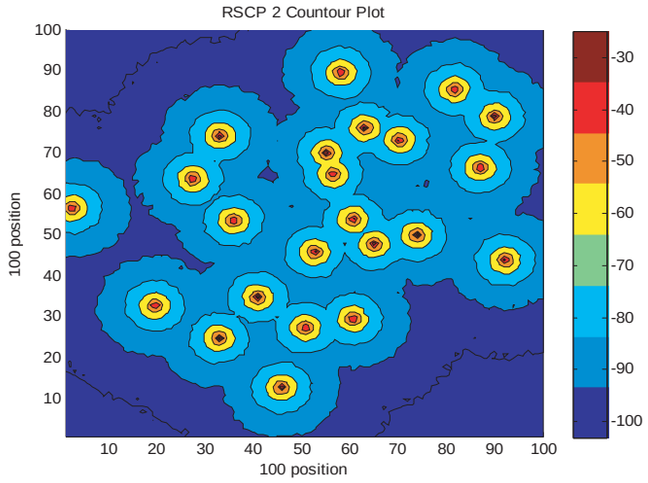

Figure 9: Predicted coverage area for COST-231 and RSCP levels

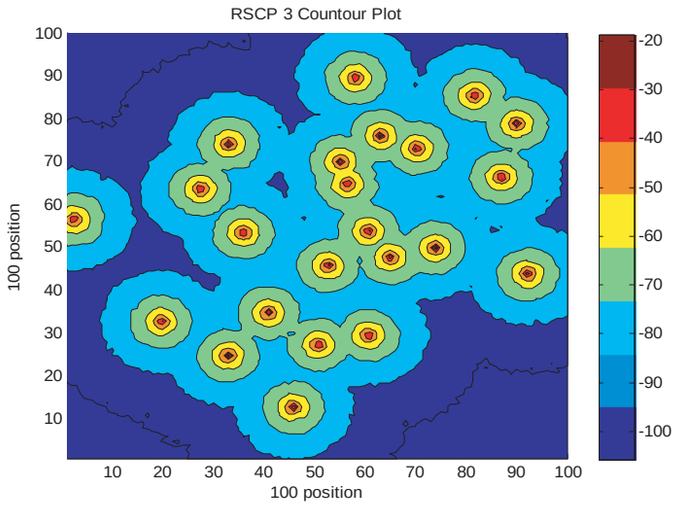

Figure 10: Predicted coverage area for COST231-WI and RSCP levels

b) New Base Station Position

To obtain maximum coverage area and minimum base station, position for four base stations have been rearranged. These base stations have filled the areas that have no base station, after which three base stations were removed from the area. Default base stations were 23 but have been reduced to 20 for the new base station positions. Whether the new base station position can obtain better coverage was observed. The former and new base station positions are shown in Figure 11.

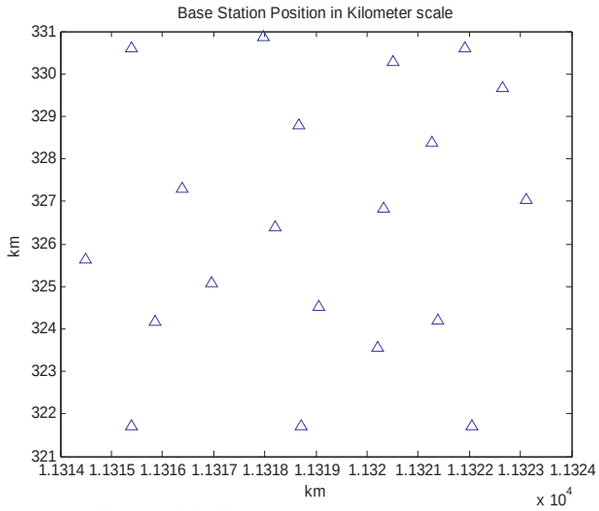

Figure 11: New base stations position

A result of predicted coverage area for new base station position is illustrated in Figure 12. The values of good RSCP have been increased for both of the propagation models, i.e. about 5 %. In this case the size of coverage area is nearly all covered up. Although numbers of base stations have been reduced, the values of finest RSCP still increased. This designates the capability of software tools in predicting the coverage area.

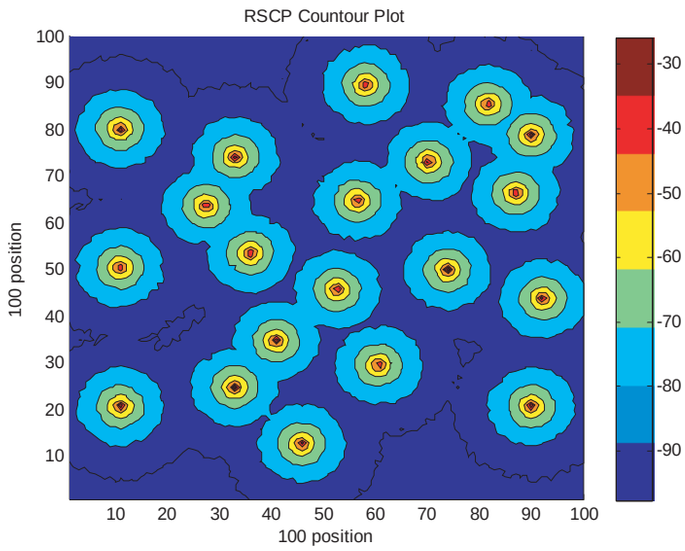

Figure 12: Predicted coverage area for new base stations position

6. CONCLUSION

Calculated signal strength (RSCP) data have been suited with actual data to gain minimum error, after which the values of RSCP have been used to predict the coverage area of Putrajaya and Cyberjaya. The software tools that have been developed can be an enhancement to achieve better coverage. Capability of software tools have been tested with improvements of base stations position. This is also called an optimisation of base station placement or coverage fine-tuning. As a conclusion, coverage prediction is important because it is required for a proper coverage planning and is a basis for the high-level network planning process.

REFERENCES

AWE Communications Software Development (2003). *COST 231 Walfisch-Ikegami Model - A fast empirical Prediction Model for Urban Scenarios*, AWE Communications. http://www.awe-communications.com/Propagation/Urban/COST/index.htm. (Last access date: 7 Jan 2008)

Casaravilla, J., Dutra, G., Pignataro, N. & Acuna J. (2003). Propagation Model for Small Macrocells in Urban Areas, M.Sc. Thesis, Universidad De La Republica, Udelar.

Chevallier, C., Brunner, C., Garavaglia, A., Murray, K. P. & Baker, K. R. (2006). WCDMA (UMTS) Deployment Handbook Planning and Optimization Aspects, John Wiley & Sons Ltd.

Dinan, E., Kurochkin, A. & Kettani, S. (2002). UMTS Radio Interface System Planning and Optimization, *Bechtel Telecomm. Techn. J.*, **1**; 21-72

GmbH Germany (2004). Chapter 4: Propagation Prediction Models, http://www.it.lut.fi/kurssit/04-05/010651000/Luennot/Chapter4.pdf (Last access date: 10 Jan 2008).

Guo, L., Zhang, J. & Maple, C. (2003). Coverage & Capacity Calculations For 3G Mobile Network Planning, in *Post Graduate Networking Conference*, http://www.globalsecurity.org/military/library/report/1990/CMG.htm (Last access date: 12 Nov 2007).

Heiska, K. (2004). On the Modelling Of WCDMA System Performance with Propagation Data, Department of Electrical and Communications Engineering, Helsinki University of Technology, Espoo, Finland.

Kandasamy, S. K., Ismail M. & Tiong S.K. (2004). Application of Genetic Algorithm for Large Scale Coverage Prediction in GSM Cellular Mobile System. *In* MMU International Symposium on Information and Communications Technologies 2004, Putrajaya, Malaysia, pp.TS6C-3 9-12.

Lempiäinen, J. & Manninen, M. (2001). Radio Interface System Planning for GSM/GPRS/UMTS, Springer Global System for Mobile Communications.

Matha, B. (1999). Radio Propagation in Cellular Networks: COST 231 Walfisch- Ikegami Model, Artech House, Boston-London, Internal Report, http://www.ee.bilkent.edu.tr/~microwave/programs/wireless/prop/costWI.htm (Last access date: 6 Jan 2008)

Matha, B. (1999). Radio Propagation in Cellular Networks: Cost 231 Hata Model, Artech House, Boston-London, Internal Report, http://www.ee.bilkent.edu.tr/~microwave/programs/wireless/prop/CostHata.htm (Last access date: 6 Jan 2008)

Nawrocki, M. J., Dohler, M. & Aghvami, A. H. (2006). Understanding UMTS Radio Network Modelling, Planning and Automated Optimisation – Theory and Practice, John Wiley & Sons, Ltd.

Niemelä, J. (2006). Aspects of Radio Network Topology Planning in Cellular WCDMA, Ph.D. Dissertation, Tampere University of Technology.

Sun Y. (2004). Radio Network Planning for 2G and 3G. Paper presented at Seminar on Topics in Communications Engineering, Master of Science in Communications Engineering, Munich University of Technology.

Zreikat, A. & Al-Begain K (2003). Simulation of 3G Networks in Realistic Propagation Environments. *Intl. J. Simulation*, **4**: 21-30.

CATCH OF THE NET

Given the rapid advancements in military technology, it is important for defence professionals, military personnel and industry specialists to keep abreast with the latest developments in the areas of defence, military and security issues. While there are hundreds of websites dealing with this, the following are relatively interesting and useful websites on defence technologies and issues:

1) DefenceTalk
http://www.defencetalk.com

The DefenceTalk website is a joint effort by users in various parts of the world who are dedicated to strategic defence, military, defence technologies, military weapons, and related issues. The website provides up-to-date international defence, military and strategic news and information, in addition to hosting a forum for extensive discussions on various defence and military issues.

2) Defense Update
http://www.defense-update.com

Defense Update highlights worldwide defense programs, including land, air, naval, C4ISR, intelligence, and net-centric warfare, infantry warfighting tactics and techniques, homeland defense etc.

3) Jane's Information Group
http://www.janes.com

The Jane's Information Group is a world leading provider of intelligence and analysis on national and international defence, security and risk developments

4) Malaysian Defence
http://www.malaysiandefence.com/

Malaysian Defence is the brainchild of Marhalim Abas, a former journalist of New Straits Times/The Malay Mail. This website focuses on defence and military issues in Malaysia.

5) Air Attack
http://www.air-attack.com

6) Alert 5
http://www.alert5.com/

7) MILAVIA
http://www.milavia.net/

Websites on military aviation news and factsheets.

8) Military Spot
http://www.militaryspot.com

A very informative military portal.